Small Molecule Disruptors of the Glucokinase–Glucokinase Regulatory Protein Interaction: 4. Exploration of a Novel Binding Pocket

14 AUTHORS, INCLUDING:

Kate S Ashton
Amgen

24 PUBLICATIONS   482 CITATIONS

SEE PROFILE

Michael Bartberger
Amgen

95 PUBLICATIONS   3,175 CITATIONS

SEE PROFILE

Samer Chmait
Amgen

17 PUBLICATIONS   192 CITATIONS

SEE PROFILE

Glenn Sivits
Amgen

11 PUBLICATIONS   498 CITATIONS

SEE PROFILE

Small Molecule Disruptors of the Glucokinase−Glucokinase Regulatory Protein Interaction: 4. Exploration of a Novel Binding Pocket

Fang-Tsao Hong,*,[†] Mark H. Norman,*,[†] Kate S. Ashton,[†] Michael D. Bartberger,[‡] Jie Chen,[§] Samer Chmait,[‡] Rod Cupples,[∥] Christopher Fotsch,[†] Steven R. Jordan,[‡] David J. Lloyd,[∥] Glenn Sivits,[∥] Seifu Tadesse,[†] Clarence Hale,[∥] and David J. St. Jean, Jr.[†]

[†]Departments of Therapeutic Discovery−Medicinal Chemistry, [‡]Therapeutic Discovery−Molecular Structure, [§]Pharmacokinetics and Drug Metabolism, and [∥]Metabolic Disorders, Amgen, Inc., One Amgen Center Drive, Thousand Oaks, California 91320-1799, United States

S *Supporting Information*

ABSTRACT: Structure−activity relationship investigations conducted at the 5-position of the *N*-pyridine ring of a series of *N*-arylsulfonyl-*N*′-2-pyridinyl-piperazines led to the identification of a novel bis-pyridinyl piperazine sulfonamide (**51**) that was a potent disruptor of the glucokinase−glucokinase regulatory protein (GK−GKRP) interaction. Analysis of the X-ray cocrystal of compound **51** bound to hGKRP revealed that

the 3-pyridine ring moiety occupied a previously unexplored binding pocket within the protein. Key features of this new binding mode included forming favorable contacts with the top face of the Ala27-Val28-Pro29 ("shelf region") as well as an edge-to-face interaction with the Tyr24 side chain. Compound **51** was potent in both biochemical and cellular assays (IC$_{50}$ = 0.005 μM and EC$_{50}$ = 0.205 μM, respectively) and exhibited acceptable pharmacokinetic properties for in vivo evaluation. When administered to *db/db* mice (100 mg/kg, po), compound **51** demonstrated a robust pharmacodynamic effect and significantly reduced blood glucose levels up to 6 h postdose.

INTRODUCTION

Glucokinase (GK), which is mainly expressed in the liver and pancreas, is the primary regulator of glucose homeostasis and is responsible for the phosphorylation of glucose to form glucose 6-phosphate (G6P).[1] While pancreatic GK plays a role in regulating insulin secretion; hepatic GK functions as an important regulator for glucose uptake, glycogen synthesis, and hepatic glucose output.[2] The activity of GK in the liver is partially controlled by glucokinase regulatory protein (GKRP).[3] During fasting, GKRP sequesters GK in the nucleus of hepatocytes and renders it inactive. When glucose levels increase by dietary intake, the GK−GKRP complex is destabilized and GK dissociates from GKRP, translocates into the cytoplasm, and initiates the hepatic glucose metabolic process.[4] Increasing GK activity through the use of glucokinase activators (GKAs) has emerged as a promising approach to treat diabetes, and several small molecules are currently under investigation in clinical trials.[5] While this strategy is attractive, there is an increased risk of hypoglycemia with the use of GKAs. One approach that has been taken to mitigate this risk has been to design hepatoselective GK activators that are taken up by the liver exclusively and thereby eliminating pancreatic GK activation.[6] We have investigated an alternative approach where GK activity is modulated through the disruption of the GK−GKRP interaction.[7−11]

In a previous report we identified compounds **1** and **2** (Figure 1) as potent and efficacious GK−GKRP disruptors through
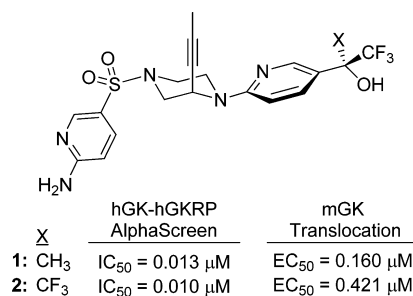

Figure 1. Piperazine-propynyl lead compounds **1** and **2**.

	X	hGK-hGKRP AlphaScreen	mGK Translocation
1:	CH$_3$	IC$_{50}$ = 0.013 μM	EC$_{50}$ = 0.160 μM
2:	CF$_3$	IC$_{50}$ = 0.010 μM	EC$_{50}$ = 0.421 μM

optimization of the *N*-aryl carbinol moiety, which we refer to as the C-ring.[11] Compounds **1** and **2** were found to potently inhibit the GK−GKRP interaction (IC$_{50}$ = 0.013 and 0.010 μM, respectively), and they effectively caused GK translocation in mouse hepatocytes (EC$_{50}$ = 0.160 and 0.421 μM, respectively). In addition, compound **1** was shown to be effective in reducing blood glucose levels in *db/db* mice (up to 70% at 100 mg/kg, po).

In our efforts to further improve the potency and increase structural diversity of this class of GK−GKRP disruptors, we examined the crystal structure of these piperazine-propynyl derivatives in more detail with the aim of identifying areas where
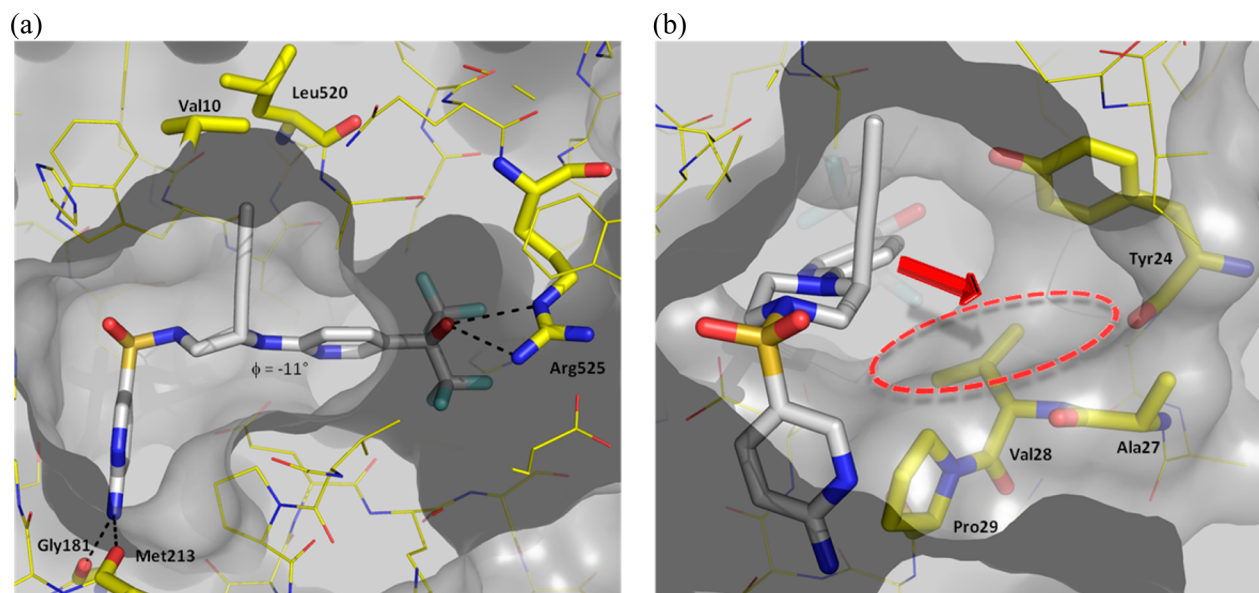
Figure 2. Model of compound **2** based on the cocrystal structure of full-length human GKRP obtained with a structurally similar compound in this series (i.e., phenyl C-ring).[10] (a) Side view illustrating the main interactions of the ligand with the protein. Note: the labeled dihedral angle is between the propynyl-bearing piperazine carbon and the pyridyl ring carbon ($\phi = -11°$). (b) Front view showing the unoccupied shelf region next to Tyr24 and above Ala27-Pro29 (highlighted by the dashed red oval). The solid red arrow indicates the proposed substitution on the 5-position of the pyridyl C-ring.

additional binding interactions might be gained.[12,13] As shown in Figure 2a, compound **2** binds to GKRP and forms key interactions with the protein in three main areas: (1) the amino group of the aminopyridine sulfonamide forms a bidentate hydrogen bonding interaction with the carbonyl groups of Gly181 and Met213; (2) the propynyl methyl group occupies a hydrophobic pocket formed by Val10 and Leu520; and (3) the bis-trifluoromethyl carbinol oxygen forms a hydrogen bonding interaction with Arg525. In addition to these three main areas, a fourth region was identified within the binding site that was not occupied by compound **2**. We refer to this area as the "shelf region" (highlighted by the red oval in Figure 2b) and is composed of the floor residues Ala27, Val28, and Pro29 and a side wall created by the π-face of the Tyr24 side chain. We postulated that an improvement in binding affinity might be achieved by targeting this unexplored pocket and that this shelf region could be accessed by substituting on the 5-position of the pyridyl C-ring of compound **2** (as indicated by the red arrow in Figure 2b). To test this hypothesis, we prepared the bis-propynyl derivative, **3** (Figure 3), and evaluated it for its ability to disrupt the hGK−hGKRP interaction.

Unfortunately, the hGK−hGKRP AlphaScreen data of compound **3** was surprisingly low (IC$_{50}$ = 8.6 μM). We speculated that this decrease in activity may be due to an unfavorable dihedral angle between the central piperazine ring

and the pyridyl carbinol C-ring since we had found from our previous structure−activity relationship (SAR) investigations that compounds that could more easily adopt a planar arrangement were preferred.[10] Therefore, to better understand the stark difference in activity between compound **2** and its bis-propynyl derivative **3**, a quantum mechanical study was performed to analyze the conformational preferences with respect to the dihedral angle between the central piperazine and the pyridine C-rings of three propynyl substituted compounds (Figure 4).[14] For computational efficiency, the carbinol moiety on the pyridyl C-ring was eliminated and a

Figure 4. Dihedral angle plot (B3LYP/6-31G* with SCRF aqueous solvation) for model substituted *N*-pyridylpiperazines. Scanned dihedral depicted in bold and defined as 0° for the depicted conformer. Each point on the plot corresponds to the lowest-energy structure arising from a full stochastic conformational search, followed by full B3LYP/6-31G* geometry optimization, each subject to the given dihedral constraint. See Supporting Information for full details.

Figure 3. Bis-propynyl derivative **3**.

generic phenyl sulfonamide was used in place of the amino-pyridine sulfonamide group.

The dihedral angle plot for the compound with the alkyne substitution only on the piperazine ring (compound (a) shown in green; Figure 4) shows that the lowest energy conformers reside between 0 and 20°; 180 and 220°; and 350 and 360° ($E_{rel} \leq 0.5$ kcal/mol; Figure 4). This is consistent with the crystallographic data, where a near-coplanar orientation (−11°) was observed for compounds similar to compound **2** in hGKRP.[10] However, the analogous coplanar conformation is highly inaccessible to compound **3** as is shown by the dihedral angle plot for the bis-propynyl substituted derivative (curve (b) in red; Figure 4). When the piperazine and the pyridyl rings of this bis-substituted compound are in a coplanar orientation, the compound resides near a maximum on its potential energy surface, approximately 2.5 kcal/mol higher in energy than its global minimum (∼60°).

In addition to examining the compounds with substitution patterns such as **2** and **3**, we also generated the dihedral angle plot of the compound containing the propynyl substitution only on the pyridyl C-ring (compound (c) shown in blue; Figure 4). Interestingly, we found that compound (c) was predicted to exhibit a similar conformational preference to that of compound (b), even in the absence of substitution on the piperazine ring, with the global minima being ∼45−65°. We attribute the significant conformational changes of (b) and (c) [versus compound (a)] to the repulsive steric interactions occurring between the propynyl group on the pyridyl C-ring and the methine hydrogen (in compound (b)) or the methylene hydrogens (in compound (c)) adjacent to the proximal piperazine nitrogen. These computational results suggest that the deviation from coplanarity predicted for (b) and (c) would prohibit access to both the upper hydrophobic pocket and the shelf regions simultaneously without engaging in a significant steric clash with the protein. This observation is consistent with the empirical result obtained for compound **3**. Therefore, to gather information solely from targeting the unexplored shelf region, we prepared and evaluated a set of compounds where the 5-position of the pyridine ring was substituted with various groups and the propynyl group on the piperazine was removed entirely (i.e., general scaffold **4**, Figure 5). We postulated that the
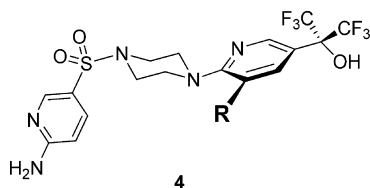

Figure 5. General scaffold **4** designed to project substituents on the pyridyl C-ring toward the targeted shelf region.

N-pyridinylpiperazine moiety of **4** would provide a conformationally rigid scaffold and project the "R" substituent on the pyridine ring toward the targeted shelf region while, at the same time, retaining a low energy conformation devoid of steric clashes in other regions of the ligand binding site.

■ CHEMISTRY

The syntheses of bis-trifluoromethylcarbinols **3** and **23−67** are outlined in Scheme 1. Commercially available 2,3-disubstituted nicotinic acids **5−7** were converted to their corresponding bis-trifluoromethylcarbinols **8−10** via a two-step sequence; first by treatment with oxalyl chloride followed by the reaction of the

resulting acyl chlorides with two equivalents of trifluoromethyl-trimethylsilane in the presence of tetramethylammonium fluoride.[15] For the synthesis of compound **3**, the chloride group at the 6-position of compound **8** was displaced with (*S*)-1-benzyl-3-(prop-1-yn-1-yl)piperazine (**11**)[16] under palladium (0)-catalyzed conditions[17] to generate the *N*-pyridinyl-*N*′-benzylpiperazine intermediate **12**, and the benzyl protecting group was removed to provide compound **13**. Treatment of intermediate **13** with *tert*-butyl (5-(chlorosulfonyl)pyridin-2-yl)carbamate **14**[16] afforded sulfonamide **15** in good yield. The second alkynyl group was introduced by the palladium-mediated coupling[18] of compound **15** with 1-propynyl trimethylsilane and subsequent removal of the *tert*-butoxycarbonyl (Boc) group gave the requisite bis-alkynyl derivative, **3**.

For the syntheses of the unsubstituted piperazine derivatives, *tert*-butyl piperazine 1-carboxylate was utilized as the nucleophilic coupling partner and was reacted with pyridinyl bis-trifluoromethylcarbinols **8−10**. The resulting *tert*-butyl carbamate protecting groups were removed to furnish intermediates **16−18**, respectively. Sulfonamide intermediates **19−21** were obtained by coupling **16−18** with sulfonyl chloride **14** in the presence of triethylamine.

The final targets (**23−67**) were prepared from intermediates **19**, **20**, or **21** by following one of two general methods: by a palladium-catalyzed coupling reaction[19] to introduce the substituent at the 5-position of the pyridine ring followed by removal of the Boc-protecting group (via **22**) or by reversing the coupling/deprotection sequence (via **23**). For Suzuki coupling reactions, the chloro and bromo intermediates (**19**, **20**, and **23**) were viable coupling partners; however, for Sonogashira-type alkynylation reactions, bromo intermediate **20** was required. Finally, the unsubstituted derivative (**26**) was prepared by palladium-mediated reduction of chloro intermediate **23** with formic acid in the presence of triethylamine.[20]

■ RESULTS AND DISCUSSION

The compounds described in this article were evaluated for their ability to disrupt the human GK−GKRP binding interaction using an in vitro AlphaScreen assay, and the data are reported in Tables 1−4.[21] The cellular activities were determined in primary mouse hepatocytes by treating the cells with test compound and measuring the difference between the nuclear and cytoplasmic GK using an Operetta platform. Compounds that were effective disruptors of the GK−GKRP interaction increased GK translocation, and therefore, decreased amounts of GK were observed in the nucleus. In addition to the biochemical binding and cellular translocation assays, the compounds were incubated in human and rat liver microsomes (HLM and RLM) for an initial assessment of oxidative metabolism. The microsomal data are reported in Tables 1−4 as intrinsic clearance (CL_{int} (μL/min/mg)), and these data were utilized to help prioritize potent compounds for further pharmacokinetic studies (vide infra).

In the initial phase of this investigation we examined a small set of analogues that contained nonaromatic substituents at the 5-position of the bistrifluoromethylcarbinol-pyridyl ring, which we refer to as the C-ring (Table 1). The unsubstituted derivative (**26**) and the halogen-substituted analogues (**23** and **24**) were modestly active in the biochemical binding assay (IC_{50} values of ∼100−200 nM), yet were fairly weak in the GK translocation assay (EC_{50} values of ≥5 μM). It is worth noting that compound **26** lost ∼18-fold activity in biochemical potency by not accessing the upper hydrophobic pocket when compared with compound **2**.[22] Compounds with small alkoxy or alkyl substituents, such as

Scheme 1. Synthesis of 2-(6-(4-((6-Aminopyridin-3-yl)sulfonyl)piperazin-1-yl)-5-substituted-pyridin-3-yl)-3-bis-trifluoromethylcarbinols[a]
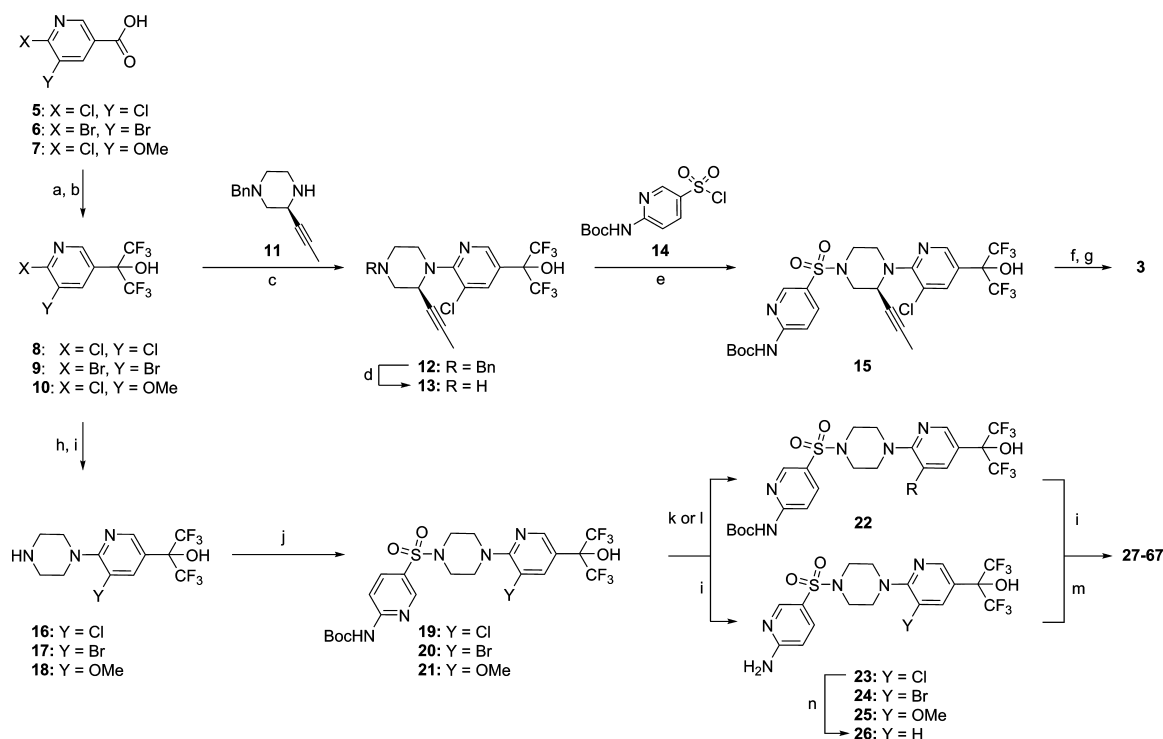
[a]Reagents and conditions: (a) oxalyl chloride, DCM, DMF, rt; (b) 2 equiv of TMSCF$_3$, Me$_4$NF, DME, −78 °C to rt; (c) from compound **8**, Ruphos, Ruphos first generation precatalyst, NaO^{t}Bu, 1,4-dioxane, 100 °C; (d) 1-chloroethyl chloroformate, K$_2$CO$_3$, DCM, rt, then MeOH, rt; (e) Et$_3$N, DCM, rt; (f) TMSCCCH$_3$, Xphos precatalyst, Cs$_2$CO$_3$, MeCN, 95 °C; (g) 4 N aq HCl, 1,4-dioxane, rt; (h) *tert*-butyl piperazine-1-carboxylate, ^{i}Pr$_2$EtN, DMF, microwave, 140 °C; (i) TFA, DCM, rt; (j) **14**, Et$_3$N, DCM, rt; (k) from compound **19** or **20**, ArB(OH)$_2$ or ArB(OR)$_2$, Pd(amphos)Cl$_2$, K$_2$CO$_3$, aq 1,4-dioxane, Δ; (l) from compound **20**, terminal alkynes, Pd(PPh$_3$)$_4$, CuI, Et$_3$N, DME, 60 °C, or Xphos precatalyst, Cs$_2$CO$_3$, MeCN, Δ; (m) from compound **23**, ArB(OH)$_2$ or ArB(OR)$_2$ (or 2-cyclopropyl-6-methyl-1,3,6,2-dioxazaborocane-4,8-dione), Pd(amphos)Cl$_2$, K$_2$CO$_3$, aq 1,4-dioxane, Δ; (n) HCO$_2$H, Et$_3$N, Pd(amphos)Cl$_2$, DMF, Δ, microwave.
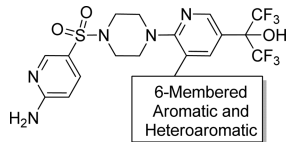
methoxy and cyclopropyl derivatives **25** and **27**, showed inferior biochemical activities; however, potency was enhanced significantly by extending further into the shelf region of the active site by the addition of alkynyl substituents to the 5-position of the pyridine ring (i.e., compounds **28**−**32**). For example, an 18-fold increase in potency was achieved when the cyclopropyl group of **27** was extended further into the pocket with an alkynyl spacer to give cyclopropylalkyne **28** (IC$_{50}$ = 0.033 μM). This result was encouraging in that this was the first compound in this series with sub-100 nM biochemical potency; however, a large cellular shift was observed in the hepatocyte assay for this particular analogue (~100-fold shift). The activities were further enhanced by either addition of a hydroxymethylene group (**29**) or a methoxy-methylene moiety (**30**) at the ethynene terminal position. However, gem-dimethyl substitution or homologation of the hydroxymethylene alkyne group in compound **29** resulted in decreased activities (compounds **31** and **32**, respectively), particularly in the cellular assay. Among these derivatives, the methylene-methoxyalkynyl analogue (**30**) was the most potent compound in both the biochemical and cellular assays (IC$_{50}$ = 0.005 μM and EC$_{50}$ = 0.254 μM, respectively), and it was over 200-fold more active than the derivative with methoxy group directly attached to the pyridine ring (**25**). Unfortunately, compound **30** showed rapid clearance in rat liver microsomes.

The shelf region SAR was expanded by preparing a small set of 5-membered aromatic heterocyclic derivatives. As shown in Table 2, the first example, 3-1H-pyrazole **33**, was only

moderately active in the biochemical binding assay. However, the 1-methyl-4-1H-pyrazole derivative (**34**) showed excellent potencies both in the biochemical and cellular assays (IC$_{50}$ = 0.001 μM; EC$_{50}$ = 0.052 μM). This exciting result prompted us to screen other N-alkyl-pyrazole derivatives. The SAR trend from the data of alkyl pyrrazoles **34**−**37** clearly revealed that steric hindrance plays an important role, as the potencies dropped with increasing size of N-alkyl group. This rank order appeared to hold as far as the metabolic stabilities were concerned as well (i.e., lower metabolic stabilities were observed from methyl (**34**) → ethyl (**35**) → iso-propyl (**36**) → tert-butyl (**37**)). Alkyl-substitutions at the position alpha to the pyrazole nitrogen were not beneficial to activity (**38** and **39**). Replacement of 1-methyl-1H-pyrazole with either 3-furan (**40**) or 4-methyl-2-thiofuran (**41**) resulted in significantly decreased potencies in the cell-based assay (EC$_{50}$ = 1.73 and 1.19 μM, respectively).

In attempts to more fully occupy the shelf region of hGKRP, we expanded our SAR studies by examining the effect of substituting 6-membered aromatic groups on the 5-position of the pyridine C-ring (Table 3). The unsubstituted phenyl analogue (**42**) potently disrupted the hGK−hGKRP interaction (IC$_{50}$ = 0.007 μM) and it also showed submicromolar activity in the cellular GK translocation assay (EC$_{50}$ = 0.776 μM). In addition, this derivative was reasonably stable in microsomes (CL$_{int}$ = 14/49 μL/min/mg in HLM/RLM), encouraging us to survey the effects of the substitutions on the aromatic ring. To gain more potency/stability insights, several substituted phenyl

Table 1. SAR of Nonaromatic Substituted Analogues 23−32

Cmpd No.	Nonaromatic Group	hGK-hGKRP AlphaScreen IC$_{50}$ (µM)^a	mGK Translocation EC$_{50}$ (µM)^b	HLM/RLM CL$_{int}$ (µL/min/mg)^{c,d}
26	H—	0.176	>12.5	<14/<14
23	Cl—	0.201	6.36	<14/26
24	Br—	0.112	5.37	<14/32
25	—O—	1.110	N/A	<14/<14
27	cyclopropyl	0.601	N/A	38/27
28	cyclopropyl-alkyne	0.033	3.35	<14/67
29	HO-alkyne	0.014	0.510	<14/65
30	—O-alkyne	0.005	0.254^e	15/399
31	HO-alkyne	0.049	2.14	<14/16
32	HO-alkyne	0.017	2.00	<14/68

^{a}AlphaScreen data reported as an average ($n \geq 3$). Standard deviations are reported in the Supporting Information. ^{b}Unless otherwise noted, $n = 1$. ^{c}In vitro microsomal stability measurements were conducted in the presence of NADPH at 37 °C for 30 min at a final compound concentration of 1 µM. ^{d}Average of 2 experimental values.

Table 2. SAR of 5-Membered Heteroaromatic Analogues 33−41

Cmpd No.	5-Membered Heteroaromatic	hGK-hGKRP AlphaScreen IC$_{50}$ (µM)^a	mGK Translocation EC$_{50}$ (µM)^b	HLM/RLM CL$_{int}$ (µL/min/mg)^{c,d}
33	H-N pyrazole	0.201	11.2	<14/20
34	N-methyl pyrazole	0.001	0.052^e	19/44
35	N-ethyl pyrazole	0.005	0.081	20/194
36	N-isopropyl pyrazole	0.023	1.08^e	38/198
37	N-tert-butyl pyrazole	0.087	2.45	86/459
38	N,C-methyl pyrazole	0.040	1.26	28/88
39	N-methyl-CF$_3$ pyrazole	30	N/A	50/121
40	furan	0.019	1.73	<14/57
41	thiophene	0.005	1.19	29/399

^{a}AlphaScreen data reported as an average ($n \geq 3$). Standard deviations are reported in the Supporting Information. ^{b}Unless otherwise noted, $n = 1$. ^{c}In vitro microsomal stability measurements were conducted in the presence of NADPH at 37 °C for 30 min at a final compound concentration of 1 µM. ^{d}Average of 2 experimental values. ^{e}n = 2.

derivatives (43−49) were synthesized and examined. For example, a series of *ortho*-, *meta*-, and *para*-fluorinated analogues (43−45, respectively) gave similar potencies in the AlphaScreen binding assay, but unfortunately cellular activity was diminished and no improvements were obtained in regards to metabolic stability. In addition to fluoro groups, we investigated polar functionalities on the phenyl ring (compounds 46−49). With the exception of the *ortho*-hydroxyl derivative (46), these polar and relatively large functionalities (sulfonamide, amide, and sulfone groups) had a negative impact on activities, and in general, microsomal stabilities also decreased.

Next we evaluated the disruption of the hGK−hGKRP interaction by compounds with 6-membered heteroaromatic substituents to the 5-position of the pyridyl C-ring (Table 3, 50−57). For the unsubstituted pyridines, the 3-pyridine derivative (51) not only displayed favorable in vitro activities, both in the biochemical and cellular assays, over its 4-aza isomer 50 but it also provided improved cellular potency (∼4 fold) and rat microsomal stability (∼2−3-fold) when compared with the phenyl analogue (42). Because of the promising activity and

metabolic stability of the 3-pyridine derivative (51), we also explored additional substitutions on the 3-pyridyl ring (i.e., fluoro-, methyl-, and methoxy-derivatives; 52−57). Unfortunately, each of the additional substituents that we examined resulted in a loss in potency (3−8-fold) in the AlphaScreen assay. In addition, losses in cellular activity were also observed by adding lipophilic fluoro- and methyl-substituents to the pyridine ring, with only the 3-methyl derivative 54 showing submicromolar activity (EC$_{50}$ = 0.794 µM). Pyridyl derivatives with polar methoxy-substituents, such as pyridines 56 and 57, lost activity as well, especially in the cellular translocation assay (EC$_{50}$ = 1.40 vs 0.205 µM for the unsubstituted pyridyl compound, 51).

Encouraged by the activity of pyridine 51, we obtained a cocrystal structure of this compound bound to hGKRP to better understand the key binding interactions between the ligand and the protein (Figure 6a). While the main anchoring hydrogen bonding interactions from the aminopyridinylsulfonamide and bis-trifluoromethylcarbinol moieties remain the same in 51 as those observed for compound 2, the 3′-pyridyl group on the 5-position of the C-ring occupies the Ala27-Val28-Pro29 shelf region as designed. The nitrogen atom of this pyridine ring

Table 3. SAR of 6-Membered Aromatic and Heteroaromatic Analogues 42−57

Cmpd No.	6-Membered Aromatic and Heteroaromatic	hGK-hGKRP AlphaScreen IC$_{50}$ (μM)[a]	mGK Translocation EC$_{50}$ (μM)[b]	HLM/RLM CL$_{int}$ (μL/min/mg)[c, d]
42		0.007	0.776	<14/49
43		0.007	0.803	<14/47
44		0.008	2.80	25/52
45		0.011	1.38	<14/40
46		0.006	0.565	22/125
47		0.309	N/A	40/81
48		0.050	0.766	17/63
49		0.042	2.95	32/103
50		0.021	0.933	15/31
51		0.005	0.205[f]	17/20
52		0.024	1.29	17/22
53		0.011	>12.5	24/19
54		0.029	0.794	37/259
55		0.040	4.68	43/182
56		0.016	1.40[e]	25/265
57		0.017	1.40	44/58

[a]AlphaScreen data reported as an average ($n \geq 3$). Standard deviations are reported in the Supporting Information. [b]Unless otherwise noted, $n = 1$. [c]In vitro microsomal stability measurements were conducted in the presence of NADPH at 37 °C for 30 min at a final compound concentration of 1 μM. [d]Average of 2 experimental values. [e]$n = 2$. [f]$n = 3$.

points toward the more polar solvent-exposed environment, while the pyridine hydrogens on the 3 and 4 positions are engaged in an edge-to-face interaction with the Tyr24 side chain. Figure 6b shows the superimposition of compounds **2** and **51** bound to GKRP, illustrating the conformational differences between these two ligands as well as some small changes in the surrounding residues of the GKRP protein. To make room for the sterically demanding 3′-pyridyl group in **51**, the central *N,N′*-disubstituted piperazine tilts away from the 3′-pyridyl moiety creating a ∼47° dihedral angle between the piperazine carbon and the pyridyl ring carbon. This result is in good agreement with the dihedral angle for the low energy conformation predicted from quantum mechanical calculations with a compound containing a 5-substituent on the pyridine C-ring (vide supra; compound (c), Figure 4). The 47° tilt observed in **51** relieves the torsional strain between the central two rings, and because there is enough vertical room in the active site, the methylene hydrogens of the piperazine ring do not clash with the ceiling residues. Furthermore, it is clear that an additional propargyl group on the piperazine ring would not be accommodated with such a twist between the rings and that a significant steric clash would result (see red arrow in Figure 6b).[23] In addition to differences observed in the conformation of the two ligands, some small changes were also noted in the GKRP protein. While most of the residues remained unchanged compared to the protein bound to compound **2**, small movements were observed in the shelf region residues upon binding to compound **51**. For example, Tyr24 moved back and Pro29 moved forward slightly to accommodate the 3′-pyridyl substituient of **51** (green vs gray, Figure 6b).[24]

Finally, we explored various [6.5]- and [5.6]-aromatic heterocyclic derivatives (**58**−**67**) to probe whether or not the substituents at the 5 position of the pyridyl ring could be extended further into the shelf region, and the data is summarized in Table 4. The first of the [6.5]-bicyclic aromatics that we examined was the benzo[b]thiophene derivative (**58**), which only showed modest biochemical activity when compared with simple substituted phenyl analogues (**42**−**45**, Table 3). Replacement of a carbon in the thiophene ring of **58** with a nitrogen atom provided the benzo[d]thiazole analogue (**59**) in which the cellular activity was dramatically improved (EC$_{50}$ = 1.15 μM). Activity in both in vitro assays was improved further with the corresponding benzo[d]oxazole derivatives **60** and **61** (0.020 and 0.015 μM in enzyme and 0.416 and 0.351 μM in cell, respectively). Oxindole analogues **62** and **63** were the most potent [6.5]-bicyclic systems that we surveyed, and they had relatively low enzyme-to-cell shifts (∼10-fold in both cases); however, these derivatives showed rapid clearance in rat liver microsomes. Unfortunately, diminished activities were obtained with other bicyclic heterocycles that we examined, such as indazoles **64** and **65**, indole **66**, and benzthiazole **67**. Of the indazole regioisomers, the more "linear" [6.5]-aromatic hetero-cycle (5-substituted 1*H*-indazole **64**, IC$_{50}$ = 0.060 μM) was better suited for engagement in the shelf region than its corresponding "angular" isomer (4-substituted 1*H*-indazole **65**, IC$_{50}$ = 1.95 μM). In addition, of the [5.6]-bicyclic derivatives, the smaller and more polar 2-benzoindole analogue (**66**) was slightly more favorable than the larger and more lipophilic, 2-benzothiophene derivative (**67**) (∼2-fold in both the enzymatic and cellular assays). The addition of the benzene ring of the benzothiophene was detrimental to activity when compared to the corresponding methyl thiophene derivative (i.e., **67** (IC$_{50}$ = 0.048 μM and EC$_{50}$ = 2.75 μM) vs **41** (Table 2; IC$_{50}$ = 0.005 μM and EC$_{50}$ = 1.19
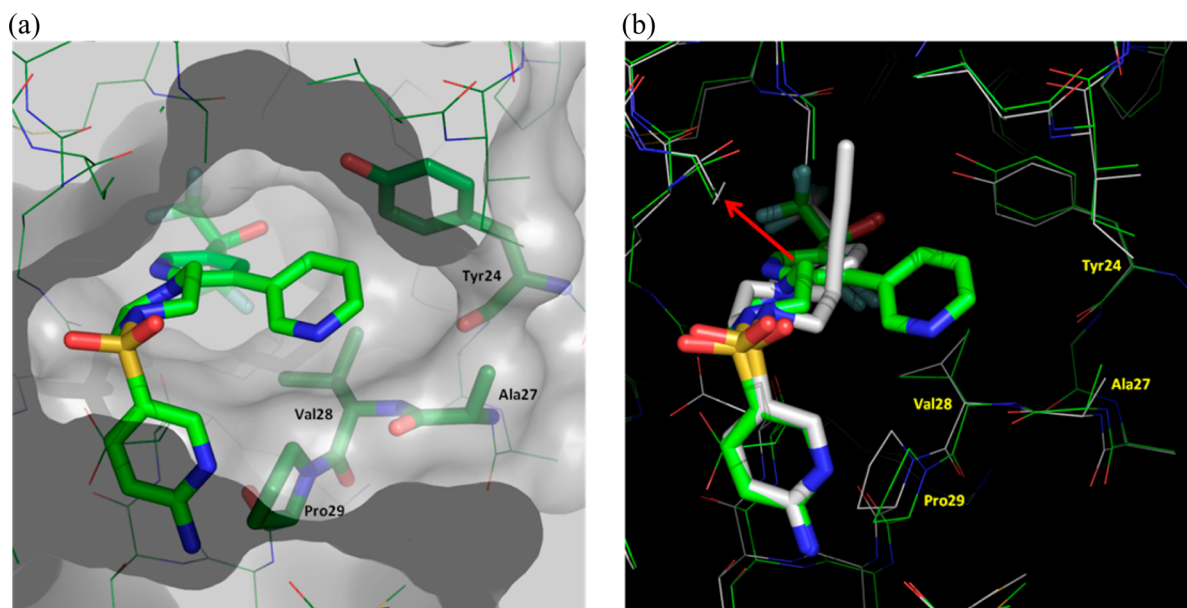
Figure 6. (a) X-ray cocrystal structure of compound **51** (green) bound to hGKRP determined at 2.20 Å resolution. The gray surface indicates the van der Waals surface area. The proteins around the targeted "shelf region" are labeled and highlighted (dark green). (b) Superimposition of compound **51** (green) with compound **2** (gray). The green hGKRP protein corresponds to compound **51**, and the gray hGKRP protein corresponds to compound **2**. The red arrow indicates the direction of the propargyl group if it were substituted on compound **51**; a steric clash with the protein would result.[22]

μM). In general, all of the bicyclic moieties that we examined showed lower metabolic stabilities, particularly in rat liver microsomes.
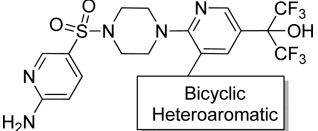
The promising in vitro potencies and stabilities of compounds **34** and **51** prompted us to evaluate their in vivo pharmacokinetic (PK) profiles (Table 5). Although there was very little difference between the pyridine **51** and methylpyrazole **34** in terms of CYP inhibition liabilities, compound **51** was found to be less protein-bound in rat plasma as compared to **34** (F_u 2.1% vs 1.1%). Pyridine **51**, which is more metabolically stable in rat liver microsomes, also showed a better overall in vivo PK profile with a lower clearance, a higher volume of distribution, and a longer mean residence time compared to methylpyrazole **34**. In addition, compound **51** was superior to **34** in an oral PK study as well, showing higher bioavailability (F = 43% vs 30%) and a greater exposure (AUC 4.74 vs 2.80 μM·h).
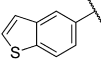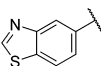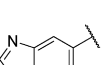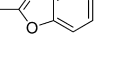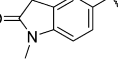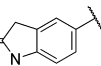
Given its encouraging in vitro cellular potency and favorable pharmacokinetic profile, pyridine **51** was evaluated further in efficacy and pharmacodynamic studies in *db/db* mice (Figure 7). In the efficacy study, **51** was administered orally to *db/db* mice at 10, 30, or 100 mg/kg, and blood glucose levels were measured at various time points (3, 6, and 24 h postdose) (Figure 7a). A statistically significant reduction in glucose levels was achieved (up to 25%) with the administration of **51** at 6 h postdose when compared to the vehicle control group.[25] In addition, the exposure of compound **51** correlated well with the amount of efficacy observed (Figure 7b). Finally, compound **51** was also examined in a pharmacodymanic assay to evaluate its ability to promote GK translocation out of the nucleus of hepatocytes at the efficacious dose in *db/db* mice. In this pharmacodymanic assay, mice were orally administered 100 mg/kg of compound **51**, and GK translocation (as determined by immunohistochemistry (IHC)) was measured in liver slices isolated at 1 and 6 h postdose. An IHC score of 0 indicated essentially complete nuclear to cytoplasmic GK translocation. Pyridine **51** produced a strong pharmacodymanic effect for up to 6 h postdose (Figure

7c), and good exposure levels were maintained during this time (Figure 7d).[26]

In summary, we have designed, synthesized, and characterized a new subseries of potent hGK−hGKRP disruptors capable of accessing a previously unexplored binding pocket in the hGKRP protein. On the basis of the *N*-pyridinylpiperazine lead compound, **2**, a systematic SAR exploration at the 5-position of the pyridine C-ring led to the discovery of **51**, which displayed favorable enzymatic and cellular potencies as well as acceptable pharmacokinetic properties. While we lost the interaction with the upper hydophobic pocket (by removing the propargyl group of compound **2**), the additional interactions that we gained by engaging the shelf region with the 3-pyrindyl group of compound **51** more than compensated for this loss. The effect on the binding contributions of the two regions can be seen by examining the activities of compound **2** (which engages the upper hydrophobic pocket), compound **51** (which engages the shelf region), and compound **26** (which does not engage either the hydrophobic pocket or the shelf region). The propargyl derivative, **2** (IC_{50} = 0.010 μM), is ∼18-fold more active than the unsusbtituted derivatve **26** (IC_{50} = 0.176 μM), while the pyridyl derivative, **51** (IC_{50} = 0.005 μM), is ∼35-fold more active than **26**. In addition to increasing potency and structural diversity, we gained an increased understanding of the conformational requirements needed for this series and have illustrated the new interactions in the Ala27-Val28-Pro29/Tyr24 shelf region (as shown in the crystal structure of compound **51** bound to hGKRP). Furthermore, compound **51** was found to be efficacious when administered orally to diabetic *db/db* mice, significantly lowering blood glucose levels at the 6 h time point. In addition to the sulfonamide compounds describe herein, a novel class of GK−GKRP disruptors that access the unique shelf-region binding pocket has also been developed, and the results will be reported in due course.

Table 4. SAR of Bicyclic Heteroaromatic Analogues 58−67

Cmpd No.	Bicyclic Heteroaromatic	hGK-hGKRP AlphaScreen IC$_{50}$ (μM)[a]	mGK Translocation EC$_{50}$ (μM)[b]	HLM/RLM CL$_{int}$ (μL/min/mg)[c, d]
58		0.047	>12.5	48/487
59		0.035	1.15	39/147
60		0.020	0.416	<14/120
61		0.015	0.351	<14/99
62		0.020	0.234	15/221
63		0.033	0.309	<14/119
64		0.060	2.63	27/88
65		1.95	N/A	42/93
66		0.027	1.12	<14/146
67		0.048	2.75	<14/315

[a]AlphaScreen data reported as an average ($n \geq 3$). Standard deviations are reported in the Supporting Information. [b]$n = 1$. [c]In vitro microsomal stability measurements were conducted in the presence of NADPH at 37 °C for 30 min at a final compound concentration of 1 μM. [d]Average of 2 experimental values.

■ EXPERIMENTAL SECTION

Biology. *hGK−hGKRP AlphaScreen, GK Translocation in Mouse Hepatocytes, and in Vivo Studies in db/db Mice.* These assays were performed as described previously.[8−10]

Measurement of B/P Ratio. Mice (CD-1) plasma and whole blood (K$_2$EDTA) were purchased from Bioreclamation. Partitioning between blood and plasma was determined in vitro using the plasma depletion assay[27] in which compound **51** levels in plasma prepared by direct addition to plasma (reference plasma) were compared with levels in plasma prepared by the addition to whole blood (sample plasma). Stock solutions of compound **51** in DMSO were first diluted by 20-fold into plasma and then diluted by 50-fold into whole blood or plasma to achieve final target concentrations of 0.1, 1.0, and 10 μM in 3 mL total volume. Samples of whole blood and plasma were gently mixed at 37 °C

Table 5. Pharmacokinetic Profiles of Selected Compounds

	in vitro properties		in vivo rat PK[a]					
	CYP inhibition	rat plasma protein binding	iv[b]			po[c]	
cmpd no.	3A4/2D6 IC$_{50}$ (μM)	F$_u$ (%)	CL (L/kg/h)	Vdss (L/kg)	MRT (h)	F (%)	AUC (μM·h)
34	27/18	1.1	2.0	2.57	1.34	30[d]	2.80[d]
51	27/27	2.1	1.5	3.36	2.18	43	4.74

[a]Pharmacokinetic parameters following administration in male Sprague−Dawley rat: unless otherwise indicated, 3 animals per study. [b]Dosed at 2 mg/kg as a solution in DMSO. [c]Dosed at 10 mg/kg as a suspension in 2% hydroxypropyl methylcellulose (HPMC), 0.1% Tween 80 pH 7 ± 1. [d]Two animals were used in this study.

for 1 h. Three equal aliquots from each concentration of whole blood and plasma were transferred to fresh tubes (0.8−1 mL). Whole blood and plasma samples were centrifuged at 2600−3000 rpm (approximately 700−1000 × *g*) for 10 min at 22 °C and after that sample plasma and reference plasma were collected. High concentration samples required dilution in plasma to bring concentrations into the dynamic range of the standard curve. Eight volumes of MeCN with internal standard were added to reference and sample plasma to precipitate protein. The reference and sample plasma samples with internal standard were centrifuged at 14,000 rpm (approximately 22,000 × *g*) for 10 min at 4 °C. The supernatants were analyzed by liquid chromatography−mass spectrometry (LC−MS).

Chemistry. *General Procedure.* Unless otherwise noted, all materials were obtained from commercial suppliers and used without further purification. Anhydrous solvents were obtained from Aldrich, Acros, or EM Science and used directly. All reactions involving air- or moisture-sensitive reagents were performed under a nitrogen or argon atmosphere. Microwave-assisted reactions were conducted either with an Initiator from Biotage, Uppsala, Sweden, or Explorer from CEM, Matthews, North Carolina. Silica gel chromatography was performed using either glass columns packed with silica gel (200−400 mesh, Aldrich Chemical) or prepacked silica gel cartridges (Biotage or Redi-Sep). Nuclear magnetic resonance (NMR) spectra were determined with a Bruker 400 MHz spectrometer. Chemical shifts are reported in parts per million (ppm, δ units). All final compounds were purified to >95% purity as determined by LC−MS obtained on an Agilent 1100 spectrometer using the following methods: [A] Agilent SB-C$_{18}$ column (50 × 3.0 mm, 2.5 μm) at 40 °C with a 1.5 mL/min flow rate using a gradient of 5−95% [0.1% TFA in MeCN] in [0.1% TFA in H$_2$O] over 3.5 min; [B] Phenomenex Gemini NX C$_{18}$ column (50 × 3.0 mm, 3 μm) at 40 °C with a 1.5 mL/min flow rate using a gradient of 5−95% [0.1% formic acid in MeCN] in [0.1% formic acid in H$_2$O] over 3.5 min. Low-resolution mass spectral (MS) data were obtained at the same time of the purity determination on the LC−MS instrument using ES ionization mode (positive).

(S)-2-(6-(4-((6-Aminopyridin-3-yl)sulfonyl)-2-(prop-1-yn-1-yl)-piperazin-1-yl)-5-(prop-1-yn-1-yl)pyridin-3-yl)-1,1,1,3,3,3-hexafluor-opropan-2-ol (3). A solution of (*S*)-*tert*-butyl (5-((4-(3-chloro-5-(1,1,1,3,3,3-hexafluoro-2-hydroxypropan-2-yl)pyridin-2-yl)-3-(prop-1-yn-1-yl)piperazin-1-yl)sulfonyl)pyridin-2-yl)carbamate (**15**) (0.100 g, 0.152 mmol), 1-(trimethylsilyl)-1-propyne (0.085 g, 0.760 mmol), Cs$_2$CO$_3$ (0.014 g, 0.456 mmol), and palladium(II) phenethylamine chloride (Xphos) (0.006 g, 7.60 μmol) in MeCN (3.0 mL) was heated to 95 °C in a sealed tube overnight. The reaction was diluted with EtOAc and H$_2$O, and the organic layer was dried over Na$_2$SO$_4$, filtered, and concentrated. The crude material was stirred in an excess amount of 4 N HCl in 1,4-dioxane for 2 h before being concentrated onto silica gel and purified by column chromatography on silica gel eluting with 0−20% (2 M NH$_3$ in MeOH) in DCM. The compound was further purified via reverse-phase preparative HPLC using a Phenomenex Gemini C$_{18}$ column (30 × 150 mm, 10 μm) eluting with 0.1% TFA in MeCN/
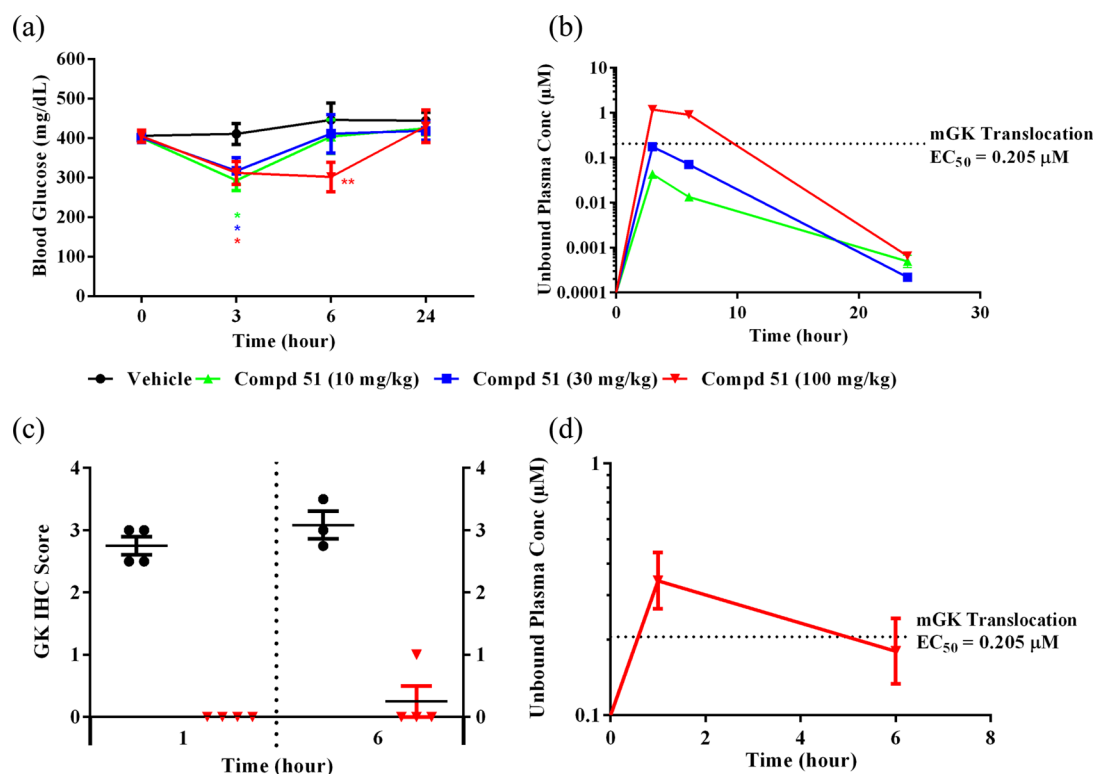
Figure 7. (a) Blood glucose measurements (3, 6, and 24 h) postoral administration of **51** (10, 30, and 100 mg/kg) to *db/db* mice. The statistical significance of the blood glucose measurements were based on comparison to the individual vehicle control groups (black, $n \geq 8$; * = $p < 0.05$, ** = $p < 0.01$, *** = $p < 0.001$). (b) Unbound plasma concentrations (3, 6, and 24 h) postoral administration of **51** (10, 30, and 100 mg/kg) to *db/db* mice. The plasma concentrations were determined based on the whole blood concentration measurements via DBS technique. (c) In vivo GK translocation in *db/db* mice following oral administration of **51** (100 mg/kg, po), $n = 4$. (d) Unbound plasma concentration of **51** from the phamacodynamic assay shown in panel c. Plasma samples were taken at terminal time points through a cardio puncture.

H_2O (20−80% over 15 min). The collected fractions were neutralized with aqueous saturated $NaHCO_3$ and extracted with EtOAc. The separated organic layer was dried over Na_2SO_4, filtered, and concentrated to give the title compound (0.015 g, 18%) as a yellow solid. MS (ESI pos. ion) m/z calcd for $C_{23}H_{21}F_6N_5O_3S$, 561; found, 562 (M + H). ^1H NMR (400 MHz, CD_3OD) δ 8.57−8.53 (m, 1H), 8.24 (d, $J = 2.3$ Hz, 1H), 8.12−8.08 (m, 1H), 7.67 (dd, $J = 2.4, 8.9$ Hz, 1H), 6.56 (d, $J = 8.8$ Hz, 1H), 4.77−4.71 (m, 1H), 4.37−4.30 (m, 1H), 3.93−3.87 (m, 1H), 3.69−3.63 (m, 1H), 3.39−3.35 (m, 2H), 2.39−2.29 (m, 1H), 2.09 (s, 3 H), 2.03 (s, 3H). Three exchangeable protons were not observed.

2-(5,6-Dichloropyridin-3-yl)-1,1,1,3,3,3-hexafluoropropan-2-ol (8). To a suspension of 5,6-dichloronicotinic acid (**5**) (3.00 g, 15.63 mmol) in DCM (20.0 mL) at room temperature was added oxalyl chloride (15.63 mL, 31.3 mmol) followed by a drop of DMF (0.1 mL). After gas evolution ceased, the solution was clear (2 h), and LC−MS showed complete conversion, the reaction was concentrated to give the crude 5,6-dichloronicotinoyl chloride (3.30 g, 100%) as an off-white solid, which was used directly without further purification.

To a suspension of the crude acyl chloride isolated above (3.30 g, 15.68 mmol) and tetramethylammonium fluoride (3.21 g, 34.50 mmol) in DME (100 mL) at −78 °C was added (trifluoromethyl)-trimethylsilane (5.10 mL, 34.50 mmol). The reaction was allowed to warm to room temperature for 1 h, then the reaction was diluted with EtOAc and aq 1 N HCl. The organic layer was separated, dried over Na_2SO_4, filtered, and concentrated. The crude material was purified by column chromatography eluting with 0−50% hexanes in EtOAc to yield the title compound (3.56 g, 72%) as an orange solid.

2-(5,6-Dibromopyridin-3-yl)-1,1,1,3,3,3-hexafluoropropan-2-ol (9). To a stirred suspension of 5,6-dibromonicotinic acid (**6**) (2.80 g, 9.97 mmol) in DCM (25.0 mL) was added oxalyl chloride (1.33 mL, 14.95 mmol), and then DMF (0.04 mL, 0.50 mmol) was slowly added at 0 °C. The foaming mixture was stirred at room temperature for 5 h and

concentrated to give the crude 5,6-dibromonicotinoyl chloride (some 5-bromo-6-chloronicotinoyl chloride was also observed) as a beige solid. DME (8.00 mL) was added to this crude material and the resulting mixture was treated with tetramethylammonium fluoride (2.01 g, 21.58 mmol) followed by the slow addition of (trifluoromethyl)-trimethylsilane (3.19 mL, 21.58 mmol) at 0 °C. The suspension was allowed to gradually warm up to room temperature and was stirred overnight. The reaction mixture was diluted with 1 N HCl (25 mL) and H_2O (15 mL) and extracted with EtOAc (3 × 35 mL). The organic extracts were washed with brine and dried over Na_2SO_4. The solution was filtered and concentrated in vacuo to give the crude material as a brown oil. This material was absorbed onto silica gel and purified by chromatography through a Redi-Sep prepacked silica gel column (40 g), eluting with a gradient of 0−30% EtOAc in hexanes, to provide a mixture of the title compound and the corresponding 2-(5-bromo-6-chloropyridin-3-yl)-1,1,1,3,3,3-hexafluoropropan-2-ol (3.83 g total) as a light-brown solid. MS (ESI pos. ion) m/z calcd for $C_8H_3Br_2F_6NO$, 403; found, 404; m/z calcd for $C_8H_3BrClF_6NO$, 359; found, 360.

2-(6-Chloro-5-methoxypyridin-3-yl)-1,1,1,3,3,3-hexafluoropropan-2-ol (10). To a stirred suspension of 6-chloro-5-methoxynicotinic acid (**7**) (0.99 g, 5.30 mmol) in DCM (5.0 mL) was added oxalyl chloride (0.71 mL, 7.95 mmol). DMF (0.021 mL, 0.27 mmol) was added slowly, and the foaming mixture was stirred at room temperature for 3 h and concentrated to give the crude acyl chloride as a beige solid. DME (8.0 mL) and tetramethylammonium fluoride (1.09 g, 11.66 mmol) were added followed by the slow addition of (trifluoromethyl)-trimethylsilane (1.73 mL, 11.66 mmol) at 0 °C. The resulting suspension was allowed to gradually warm up to room temperature and stirred overnight. The reaction mixture was diluted with aq 1 N HCl (15 mL) and H_2O (10 mL) and extracted with EtOAc (3 × 25 mL). The organic extracts were washed with 1 N NaOH (1 × 10 mL) and brine and dried over Na_2SO_4. The solution was filtered and concentrated in vacuo to give the crude material as a brown oil. The material was

absorbed onto silica gel and purified by chromatography through a Redi-Sep prepacked silica gel column (40 g), eluting with a gradient of 0−30% EtOAc in hexanes, to provide the title compound (0.97 g, 59% yield) as an off-white solid.

(S)-2-(6-(4-Benzyl-2-(prop-1-yn-1-yl)piperazin-1-yl)-5-chloropyridin-3-yl)-1,1,1,3,3,3-hexafluoropropan-2-ol (12). A solution of (S)-1-benzyl-3-(prop-1-yn-1-yl)piperazine (**11**)[16] (1.00 g, 4.67 mmol), 2-(5,6-dichloropyridin-3-yl)-1,1,1,3,3,3-hexafluoropropan-2-ol (**8**) (1.47 g, 4.67 mmol), Ruphos precatalyst (0.19 g, 0.233 mmol), Ruphos (0.11 g, 0.233 mmol), and NaO^{t}Bu (1.35 g, 14.0 mmol) in 1,4-dioxane (10.0 mL) was heated in a sealed tube at 100 °C for 30 min. The reaction was diluted with H$_2$O and extracted with EtOAc. The organic layer was dried over Na$_2$SO$_4$, filtered, and concentrated. The crude material was purified by column chromatogrpahy eluting with 0−100% EtOAc in hexanes to give the title compound (0.98 g, 43%).

(S)-2-(5-Chloro-6-(2-(prop-1-yn-1-yl)piperazin-1-yl)pyridin-3-yl)-1,1,1,3,3,3-hexafluoropropan-2-ol (13). To a suspension of (S)-2-(6-(4-benzyl-2-(prop-1-yn-1-yl)piperazin-1-yl)-5-chloropyridin-3-yl)-1,1,1,3,3,3-hexafluoropropan-2-ol (**12**) (0.98 g, 1.992 mmol) and K$_2$CO$_3$ (0.55 g, 3.98 mmol) in DCM (20.0 mL) at room temperature was added 1-chloroethyl chloroformate (0.65 mL, 5.98 mmol). After 30 min the reaction was filtered and concentrated. MeOH (20.0 mL) was added to the resulting oil, and the solution was stirred at room temperature overnight. The reaction was then concentrated to yield the title compound (0.80 g, 100%) as an oil that was used directly in the next reaction.

(S)-tert-Butyl (5-((4-(3-chloro-5-(1,1,1,3,3,3-hexafluoro-2-hydroxypropan-2-yl)pyridin-2-yl)-3-(prop-1-yn-1-yl)piperazin-1-yl)sulfonyl)pyridin-2-yl)carbamate (15). To a solution of (S)-2-(5-chloro-6-(2-(prop-1-yn-1-yl)piperazin-1-yl)pyridin-3-yl)-1,1,1,3,3,3-hexafluoropropan-2-ol (**13**) (0.80 g, 1.99 mmol) and Et$_3$N (0.83 mL, 5.97 mmol) in DCM (10.0 mL) at room temperature was added *tert*-butyl (5-(chlorosulfonyl)pyridin-2-yl)carbamate (**14**)[16] (0.64 g, 2.19 mmol). After 10 min the reaction was quenched with the addition of H$_2$O and extracted with DCM. The organic layer was dried over Na$_2$SO$_4$, filtered, and concentrated. The residue was purified by column chromatography eluting with 0−40% EtOAc in hexanes to yield the title compound (0.90 g, 69%) as a light-yellow solid.

2-(5-Chloro-6-(piperazin-1-yl)pyridin-3-yl)-1,1,1,3,3,3-hexafluoropropan-2-ol (16). A 400 mL sealable vessel was charged with 2-(5,6-dichloropyridin-3-yl)-1,1,1,3,3,3-hexafluoropropan-2-ol (**8**) (43.5 g, 139 mmol), *tert*-butyl piperazine-1-carboxylate (31.0 g, 166 mmol), DMF (100.0 mL), and ^{i}Pr$_2$EtN (36.3 mL, 208 mmol). The vessel was sealed and heated at 100 °C overnight. After the mixture was allowed to cool to room temperature, the reaction was poured into H$_2$O (750 mL). The resulting solid was collected and recrystallized from ^{i}PrOH to give *tert*-butyl 4-(3-chloro-5-(1,1,1,3,3,3-hexafluoro-2-hydroxypropan-2-yl)-pyridin-2-yl)piperazine-1-carboxylate (37.5 g, 58% yield) as a white solid.

A solution of *tert*-butyl 4-(3-chloro-5-(1,1,1,3,3,3-hexafluoro-2-hydroxypropan-2-yl)pyridin-2-yl)piperazine-1-carboxylate (5.0 g, 10.78 mmol) in DCM (20.0 mL) and TFA (20.0 mL, 269 mmol) was stirred at room temperature for 20 min. The reaction was quenched with excess solid NaHCO$_3$ and diluted with EtOAc and H$_2$O. The organic layer was separated, dried over Na$_2$SO$_4$, filtered, and concentrated. The title compound (**16**) (3.9 g, 100%) was used in the next reaction without further purification.

tert-Butyl (5-((4-(3-bromo-5-(1,1,1,3,3,3-hexafluoro-2-hydroxypropan-2-yl)pyridin-2-yl)piperazin-1-yl)sulfonyl)pyridin-2-yl)carbamate (20). To a mixture of 2-(5,6-dibromopyridin-3-yl)-1,1,1,3,3,3-hexafluoropropan-2-ol (**9**) (3.83 g, mixture with 2-(5-bromo-6-chloropyridin-3-yl)-1,1,1,3,3,3-hexafluoropropan-2-ol) and *tert*-butyl piperazine-1-carboxylate (1.59 g, 8.54 mmol) in DMF (1.0 mL) was added ^{i}Pr$_2$EtN (1.86 mL, 10.7 mmol), and the reaction mixture was stirred and heated in a microwave reactor at 140 °C for 40 min. After allowing to cool to room temperature, the mixture was added to ice−water, and the resulting precipitate was filtrated and dried under vacuum to provide crude *tert*-butyl 4-(3-bromo-5-(1,1,1,3,3,3-hexafluoro-2-hydroxypropan-2-yl)pyridin-2-yl)piperazine-1-carboxylate (2.92 g, 58% from **6**) as an off-white solid.

To a stirred mixture of *tert*-butyl 4-(3-bromo-5-(1,1,1,3,3,3-hexafluoro-2-hydroxypropan-2-yl)pyridin-2-yl)piperazine-1-carboxylate (1.62 g, 3.19 mmol) in DCM (3.0 mL) was added TFA (3.0 mL), and the mixture was stirred at room temperature for 1 h and concentrated. The mixture was concentrated and then diluted with H$_2$O (5 mL) and then aq 1 N NaOH was added carefully until neutral. The resulting beige precipitate was collected and dried. The aqueous solution was extracted with EtOAc (2 × 50 mL) and washed with brine. The organic phases were dried over Na$_2$SO$_4$ and concentrated. The solids were combined to give 2-(5-bromo-6-(piperazin-1-yl)pyridin-3-yl)-1,1,1,3,3,3-hexafluoropropan-2-ol (**17**). To the crude solid (**17**) was added DCM (30.0 mL) followed by Et^{i}Pr$_2$N (1.11 mL, 0.286 mmol) and *tert*-butyl (5-(chlorosulfonyl)pyridin-2-yl)carbamate (**14**)[16] (1.12 g, 3.820 mmol) subsequently at room temperature. The mixture was stirred at 1 h and quenched with saturated aqueous NH$_4$Cl (30 mL) and H$_2$O (50 mL). The separated aqueous layer was extracted with DCM (3 × 50 mL). The organic extracts were washed with brine and dried over Na$_2$SO$_4$. The solution was filtered and concentrated in vacuo to give the crude material as a yellow solid. The residue was absorbed onto silica gel and purified by chromatography through a Redi-Sep prepacked silica gel column (80 g), eluting with a gradient of 0−30% 2 M NH$_3$·MeOH in DCM, to provide the title compound (1.97 g, 93% yield) as a pale-yellow solid. MS (ESI pos. ion) *m/z* calcd for C$_{22}$H$_{24}$BrF$_6$N$_5$O$_5$S, 663; found, 664 (M + H).

2-(6-(4-((6-Aminopyridin-3-yl)sulfonyl)piperazin-1-yl)-5-chloropyridin-3-yl)-1,1,1,3,3,3-hexafluoropropan-2-ol (23). To a solution of 2-(5-chloro-6-(piperazin-1-yl)pyridin-3-yl)-1,1,1,3,3,3-hexafluoropropan-2-ol (**16**) (3.90 g, 10.72 mmol) and Et$_3$N (5.98 mL, 42.90 mmol) in DCM (30.0 mL) at room temperature was added *tert*-butyl (5-(chlorosulfonyl)pyridin-2-yl)carbamate (**14**)[16] (3.45 g, 11.80 mmol). After 10 min the reaction was diluted with H$_2$O and DCM, and the organic layer was separated, dried over Na$_2$SO$_4$, filtered, and concentrated. The resulting residue was dissolved in DCM (30 mL) and TFA (0.836 mL, 10.72 mmol) and stirred at room temperature for 20 min. The reaction was not complete, so 5 more equivalents of TFA was added, and complete conversion was observed after an additional 20 min. The reaction was quenched with solid NaHCO$_3$ and diluted with DCM and H$_2$O. The organic layer was separated, dried over Na$_2$SO$_4$, filtered, and concentrated to give a pale-yellow foam. This material was slurried with DCM and filtered, and 2-(6-(4-((6-aminopyridin-3-yl)sulfonyl)piperazin-1-yl)-5-chloropyridin-3-yl)-1,1,1,3,3,3-hexafluoropropan-2-ol (**23**) (1.50 g, 27%) was obtained as an off-white solid. MS (ESI pos. ion) *m/z* calcd for C$_{17}$H$_{16}$ClF$_6$N$_5$O$_3$S, 519; found, 520 (M + H). ^{1}H NMR (400 MHz, CD$_3$OD) δ 8.47−8.39 (m, 1H), 8.33−8.28 (m, 1H), 7.95−7.89 (m, 1H), 7.83 (dd, J = 2.3, 9.0 Hz, 1H), 6.75 (d, J = 9.0 Hz, 1H), 3.58−3.50 (m, 4H), 3.23−3.16 (m, 4H). Three exchangeable protons were not observed.

2-(6-(4-((6-Aminopyridin-3-yl)sulfonyl)piperazin-1-yl)-5-bromopyridin-3-yl)-1,1,1,3,3,3-hexafluoropropan-2-ol (24). To a stirred mixture of *tert*-butyl (5-((4-(3-bromo-5-(1,1,1,3,3,3-hexafluoro-2-hydroxypropan-2-yl)pyridin-2-yl)piperazin-1-yl)sulfonyl)pyridin-2-yl)-carbamate (**20**) (0.020 g, 0.03 mmol) in DCM (1.0 mL) was added TFA (1.0 mL) at room temperature, and the yellow solution was stirred for 30 min and concentrated. The crude material was dissolved in 5% 2 M NH$_3$·MeOH in DCM, absorbed onto silica gel, and purified by chromatography through a Redi-Sep prepacked silica gel column (4 g), eluting with a gradient of 0−30% 2 M NH$_3$·MeOH in DCM, to provide the title compound (0.017 g, quantitative) as a white solid. MS (ESI pos. ion) *m/z* calcd for C$_{17}$H$_{16}$BrF$_6$N$_5$O$_3$S, 563; found, 564 (M + H). ^{1}H NMR (400 MHz, DMSO-d_6) δ 9.09 (s, 1H), 8.47 (s, 1H), 8.25 (d, J = 2.35 Hz, 1H), 8.11−8.00 (m, 1H), 7.66 (dd, J = 2.45, 8.90 Hz, 1H), 7.03 (s, 2H), 6.55 (d, J = 8.80 Hz, 1H), 3.35−3.52 (m, 4H), 3.03 (br s, 4H).

2-(6-(4-((6-Aminopyridin-3-yl)sulfonyl)piperazin-1-yl)-5-methoxypyridin-3-yl)-1,1,1,3,3,3-hexafluoropropan-2-ol (25). A glass microwave reaction vessel was charged with 2-(6-chloro-5-methoxypyridin-3-yl)-1,1,1,3,3,3-hexafluoropropan-2-ol (**10**) (0.118 g, 0.381 mmol), *tert*-butyl piperazine-1-carboxylate (0.078 g, 0.419 mmol), and ^{i}Pr$_2$EtN (0.100 mL, 0.572 mmol) in DMF (0.2 mL). The reaction mixture was stirred and heated in a microwave reactor at 140 °C for 100 min and then 160 °C for 30 min. After the mixture was allowed to cool to room

temperature, H₂O was added, and the resulting precipitate was collected, washed with H₂O, and dried under vacuum to give *tert*-butyl 4-(5-(1,1,1,3,3,3-hexafluoro-2-hydroxypropan-2-yl)-3-methoxypyridin-2-yl)-piperazine-1-carboxylate (98 mg, 56%) as an off-white solid. This material was dissolved in DCM (2.0 mL), and then TFA (2.0 mL) was added at room temperature. The yellow solution was stirred at room temperature for 30 min and concentrated to give the crude 4-(5-(1,1,1,3,3,3-hexafluoro-2-hydroxypropan-2-yl)-3-methoxypyridin-2-yl)-piperazine (**18**). MS (ESI pos. ion) m/z calcd for $C_{13}H_{15}F_6N_3O_2$, 359; found, 360 (M + H).

The crude material (**18**) isolated above was dissolved in DCM (1.0 mL), and $^iPr_2EtN$ (0.041 g, 0.320 mmol) and *tert*-butyl (5-(chlorosulfonyl)pyridin-2-yl)carbamate (**14**)[16] (0.125 g, 0.427 mmol) were added. The mixture was stirred at room temperature for 1 h and concentrated to give the crude material *tert*-butyl (5-((4-(5-(1,1,1,3,3,3-hexafluoro-2-hydroxypropan-2-yl)-3-methoxypyridin-2-yl)piperazin-1-yl)sulfonyl)pyridin-2-yl)carbamate (**21**). DCM (2.0 mL) and TFA (2.0 mL) were added, and the resulting yellow solution was stirred at room temperature for 30 min. The solution was concentrated and the resulting residue was dissolved in 5% 2 M NH₃·MeOH in DCM, absorbed onto silica gel, and purified by chromatography through a Redi-Sep prepacked silica gel column (12 g), eluting with a gradient of 0–7% 2 M NH₃·MeOH in DCM, to provide the title compound (0.004 g, 2% overall yield from **10**) as a white solid. MS (ESI pos. ion) m/z calcd for $C_{18}H_{19}F_6N_5O_4S$, 515; found, 516 (M + H). ¹H NMR (400 MHz, DMSO-d_6) δ 8.80 (s, 1H), 8.22 (d, J = 2.15 Hz, 1H), 7.99 (s, 1H), 7.63 (dd, J = 2.54, 8.80 Hz, 1H), 7.30 (s, 1H), 7.03 (s, 2H), 6.53 (d, J = 8.41 Hz, 1H), 3.79 (s, 3H), 3.50–3.44 (m, 4H), 3.00–2.91 (m, 4H).

2-(6-(4-((6-Aminopyridin-3-yl)sulfonyl)piperazin-1-yl)pyridin-3-yl)-1,1,1,3,3,3-hexafluoropropan-2-ol (26). To a mixture of 2-(6-(4-((6-aminopyridin-3-yl)sulfonyl)piperazin-1-yl)-5-chloropyridin-3-yl)-1,1,1,3,3,3-hexafluoropropan-2-ol (**23**) (0.057 g, 0.11 mmol) and Pd(amphos)Cl₂ (0.004 g, 5.48 μmol) was added Et₃N (76 μL, 0.55 mmol), DMF (0.5 mL), and HCO₂H (13 μL, 0.33 mmol). The reaction mixture was stirred and heated in a microwave reactor at 120 °C for 90 min. After the solution was allowed cooled to room temperature, the mixture was diluted with saturated aqueous NH₄Cl (5 mL) and extracted with EtOAc (3 × 30 mL). The combined organic extracts were washed with brine (1 × 20 mL) and dried over Na₂SO₄. The solution was filtered and concentrated in vacuo to give the crude material as a light-yellow oil. The crude product was absorbed onto silica gel and purified by chromatography through a Redi-Sep prepacked silica gel column (12 g), eluting with a gradient of 0–70% EtOAc in hexanes, to yield the title compound (0.010 g, 18%) as a white solid. MS (ESI pos. ion) m/z calcd for $C_{17}H_{17}F_6N_5O_3S$, 485; found, 486 (M + H). ¹H NMR (400 MHz, DMSO-d_6) δ 8.61 (s, 1H), 8.31 (d, J = 2.35 Hz, 1H), 8.22 (d, J = 2.35 Hz, 1H), 7.69 (d, J = 10.76 Hz, 1H), 7.62 (dd, J = 2.54, 9.00 Hz, 1H), 6.98 (s, 2H), 6.91 (d, J = 9.19 Hz, 1H), 6.51 (d, J = 8.41 Hz, 1H), 3.73–3.59 (m, 4H), 2.95 (t, J = 4.89 Hz, 4H).

2-(6-(4-((6-Aminopyridin-3-yl)sulfonyl)piperazin-1-yl)-5-cyclopropylpyridin-3-yl)-1,1,1,3,3,3-hexafluoropropan-2-ol (27). This material was prepared according to the general procedure described for the synthesis of **26** from **23** using 2-cyclopropyl-6-methyl-1,3,6,2-dioxazaborocane-4,8-dione (0.028 g, 0.144 mmol). The reaction was heated to 120 °C for 60 h, and the crude product was purified by column chromatography eluting with 0–7% MeOH in DCM. The material was further purified via reverse-phase preparative HPLC using a Phenomenex Gemini C₁₈ column (30 × 150 mm, 10 μm) eluting with 0.1% TFA in MeCN/H₂O (10–80% over 15 min) followed by column chromatography on silica gel eluting with 0–100% EtOAc in hexanes to give the title compound (0.005 g, 7%) as a colorless film. MS (ESI pos. ion) m/z calcd for $C_{20}H_{21}F_6N_5O_3S$, 525; found, 526 (M + H). ¹H NMR (400 MHz, CD₃OD) δ 8.33–8.29 (m, 2H), 7.75 (dd, J = 2.4, 8.9 Hz, 1H), 7.50–7.45 (m, 1H), 6.64 (d, J = 9.0 Hz, 1H), 3.49–3.42 (m, 4H), 3.24–3.16 (m, 4H), 2.01–1.91 (m, 1H), 1.10–1.03 (m, 2H), 0.72–0.64 (m, 2H). Three exchangeable protons were not observed.

2-(6-(4-((6-Aminopyridin-3-yl)sulfonyl)piperazin-1-yl)-5-(cyclopropylethynyl)pyridin-3-yl)-1,1,1,3,3,3-hexafluoropropan-2-ol (28). In a 10 mL sealable tube was added *tert*-butyl (5-((4-(3-bromo-5-(1,1,1,3,3,3-hexafluoro-2-hydroxypropan-2-yl)pyridin-2-yl)piperazin-1-

yl)sulfonyl)pyridin-2-yl)carbamate (**20**) (0.040 g, 0.06 mmol) and DMF (0.5 mL). The solution was purged with argon for 15 min, and ethynylcyclopropane (1.5 equiv), Pd(PPh₃)₄ (0.003g, 0.003 mmol), Et₃N (0.041 mL, 0.300 mmol), and CuI (0.001 g, 0.006 mmol) were added. After the additions were completed, the reaction mixture was purged again with argon for 15 min, sealed, and stirred at ambient temperature for 12 h. The reaction was quenched with an excess of ice/H₂O (10 mL), and the product was extracted with EtOAc (2 × 10 mL). The organic layers were separated, dried over anhydrous Na₂SO₄, filtered, and evaporated under reduced pressure. The crude material was purified by column chromatography (100–200 silica gel) eluting with 20–27% EtOAc in hexanes to give an off-white solid, which was dissolved in DCM (1.0 mL). The resulting solution was cooled to 0 °C, and TFA (0.5 mL) was added dropwise. The reaction was stirred at ambient temperature for 2 h until the deprotection was complete as indicated by TLC (50% EtOAc/hexanes). The reaction mixture was diluted with DCM (10 mL), basified with saturated aqueous NaHCO₃, and extracted with EtOAc (10 mL). The organic layer was washed with H₂O (2 × 10 mL) and brine (10 mL) then separated, dried over Na₂SO₄, and concentrated to give the title compound (0.030 g, 37%) as an off-white solid. MS (ESI pos. ion) m/z calcd for $C_{22}H_{21}F_6N_5O_3S$, 549; found, 550 (M + H). ¹H NMR (400 MHz, DMSO-d_6) δ 8.61 (s, 1H), 8.29 (d, J = 2.4 Hz, 1H), 8.22 (d, J = 2.4 Hz, 1H), 7.70 (d, J = 2 Hz, 1H), 7.64 (dd, J = 2.4, 8.8 Hz, 1H), 7.03 (s, 1H), 6.53 (d, J = 8.8 Hz, 1H), 3.63–3.62 (m, 4H), 2.96–2.95 (m, 4H), 1.57–1.56 (m, 1H), 0.91–0.88 (m, 2H), 0.70–0.67 (m, 2H). One exchangeable proton was not observed.

3-(2-(4-((6-Aminopyridin-3-yl)sulfonyl)piperazin-1-yl)-5-(1,1,1,3,3,3-hexafluoro-2-hydroxypropan-2-yl)pyridin-3-yl)prop-2-yn-1-ol (29). This material was prepared according to the general procedure described for the synthesis of **28** from **20** (0.100 g, 0.150 mmol) using prop-2-yn-1-ol (0.013 g, 0.226 mmol) and isolated (0.030 g, 37%) as an off-white solid. MS (ESI pos. ion) m/z calcd for $C_{20}H_{19}F_6N_5O_4S$, 539; found, 540 (M + H). ¹H NMR (400 MHz, DMSO-d_6) δ 8.39 (d, J = 2.4 Hz, 1H), 8.30 (d, J = 2 Hz, 1H), 7.88 (d, J = 2 Hz, 1H), 7.75 (dd, J = 2.8, 9.2 Hz, 1H), 6.65 (d, J = 8.8 Hz, 1H), 4.43 (s, 2H), 3.78–3.76 (m, 4H), 3.16–3.14 (m, 4H). Four exchangeable protons were not observed.

2-(6-(4-((6-Aminopyridin-3-yl)sulfonyl)piperazin-1-yl)-5-(3-methoxyprop-1-yn-1-yl)pyridin-3-yl)-1,1,1,3,3,3-hexafluoropropan-2-ol (30). To a mixture of *tert*-butyl (5-((4-(3-bromo-5-(1,1,1,3,3,3-hexafluoro-2-hydroxypropan-2-yl)pyridin-2-yl)piperazin-1-yl)-sulfonyl)pyridin-2-yl)carbamate (**20**) (0.059 g, 0.089 mmol), palladium(II) phenethylamine chloride (Xphos) (0.066 g, 0.089 mmol), and Cs₂CO₃ (0.203 g, 0.622 mmol) was added methyl propargyl ether (0.037 mL, 0.444 mmol) and MeCN (1.0 mL). The mixture was stirred at 80 °C overnight, the reaction mixture was allowed to cool to room temperature, and the mixture was passed through a plug of Celite. The filter cake was washed with EtOAc and DCM (3 × 10 mL each). The combined organic phases were concentrated to give a crude residue, which was dissolved in DCM (1 mL). TFA (1 mL) was added, and the yellow solution was stirred at room temperature for 30 min then concentrated. The crude material was dissolved in 5% 2 M NH₃·MeOH in DCM and absorbed onto silica gel and purified by chromatography through a Redi-Sep prepacked silica gel column (12 g), eluting with a gradient of 0–30% 2 M NH₃·MeOH in DCM. The material was purified further by a preparative TLC purification (EtOAc/DCM, 2:3) to provide the title compound (0.002 g, 5%) as a white solid. MS (ESI pos. ion) m/z calcd for $C_{21}H_{21}F_6N_5O_4S$, 553; found, 554 (M + H). ¹H NMR (400 MHz, CD₃OD) δ 8.42 (d, J = 1.96 Hz, 1H), 8.32 (d, J = 2.15 Hz, 1H), 7.91 (d, J = 2.15 Hz, 1H), 7.75 (dd, J = 2.45, 8.90 Hz, 1H), 6.66 (d, J = 8.80 Hz, 1H), 4.37 (s, 2H), 3.81–3.73 (m, 4H), 3.41 (s, 3H), 3.20–3.12 (m, 4H). Three exchangeable protons were not observed.

4-(2-(4-((6-Aminopyridin-3-yl)sulfonyl)piperazin-1-yl)-5-(1,1,1,3,3,3-hexafluoro-2-hydroxypropan-2-yl)pyridin-3-yl)-2-methylbut-3-yn-2-ol (31). This material was prepared according to the general procedure described for the synthesis of **28** from **20** (0.100 g, 0.150 mmol) using 2-methylbut-3-yn-2-ol (0.019 g, 0.223 mmol) and isolated (0.009 g, 11%) as an off-white solid. MS (ESI pos. ion) m/z calcd for $C_{22}H_{23}F_6N_5O_4S$, 567; found, 568 (M + H). ¹H NMR (400

MHz, DMSO-d_6) δ 8.39 (d, J = 2.4 Hz, 1H), 8.30 (d, J = 2.4 Hz, 1H), 7.85 (d, J = 2.4 Hz, 1H), 7.75 (dd, J = 2.4, 8.8 Hz, 1H), 6.65 (d, J = 8.8 Hz, 1H), 3.76−3.74 (m, 4H), 3.16−3.14 (m, 4H), 1.54 (s, 6H). Four exchangeable protons were not observed.

4-(2-(4-((6-Aminopyridin-3-yl)sulfonyl)piperazin-1-yl)-5-(1,1,1,3,3,3-hexafluoro-2-hydroxypropan-2-yl)pyridin-3-yl)but-3-yn-1-ol (32). This material was prepared according to the general procedure described for the synthesis of **28** from **20** (0.100 g, 0.150 mmol) using but-3-yn-1-ol (0.016 mg, 0.226 mmol) and isolated (0.007 g, 8%) as an off-white solid. MS (ESI pos. ion) m/z calcd for $C_{21}H_{21}F_6N_5O_4S$, 553; found, 554 (M + H). ^{1}H NMR (400 MHz, DMSO-d_6) δ 8.36 (d, J = 2.8 Hz, 1H), 8.31 (d, J = 2.4 Hz, 1H), 7.86 (d, J = 2 Hz, 1H), 7.77 (dd, J = 2.4, 6.4 Hz, 1H), 6.67 (d, J = 9.2 Hz, 1H), 3.79−3.77 (m, 6H), 3.16 (t, J = 5.2 Hz, 4H), 2.38 (t, J = 6.4 Hz, 2H). Four exchangeable protons were not observed.

2-(6-(4-((6-Aminopyridin-3-yl)sulfonyl)piperazin-1-yl)-5-(1H-pyrazol-3-yl)pyridin-3-yl)-1,1,1,3,3,3-hexafluoropropan-2-ol (33). A solution of *tert*-butyl (5-((4-(3-bromo-5-(1,1,1,3,3,3-hexafluoro-2-hydroxypropan-2-yl)pyridin-2-yl)piperazin-1-yl)sulfonyl)pyridin-2-yl)-carbamate (**20**) (0.100 g, 0.151 mmol), (1H-pyrazol-3-yl)boronic acid (0.034 g, 0.301 mmol), Pd(amphos)Cl$_2$ (0.005 g, 0.008 mmol), and K$_2$CO$_3$ (0.062 g, 0.452 mmol) in 1,4-dioxane (5.0 mL) and H$_2$O (0.2 mL) was heated in a sealed tube at 120 °C overnight. The reaction mixture was allowed to cool to room temperature and then passed through a short path of Celite. The filter cake was washed with EtOAc and DCM (3 × 25 mL each). The filtrate was concentrated in vacuo, the residue was treated with DCM (10 mL) and TFA (10 mL), and the mixture was stirred for 1 h. The solution was concentrated, and the crude residue was purified using Xbridge 19 × 100 mm, 10 μm Column, 40 mL/min flow rate, 0.1% TFA in H$_2$O/MeCN. The TFA salt of the title compound was isolated (0.056 g, 56%) as a tan solid. MS (ESI pos. ion) m/z calcd for $C_{20}H_{19}F_6N_7O_3S$, 551; found, 552 (M + H). ^{1}H NMR (400 MHz, DMSO-d_6) δ 9.03−8.69 (m, 1H), 8.41 (d, J = 2.35 Hz, 1H), 8.28 (br s, 1H), 8.06 (s, 1H), 7.77 (d, J = 2.15 Hz, 2H), 7.57 (s, 2H), 6.78 (d, J = 7.43 Hz, 1H), 6.75−6.68 (m, 1H), 6.61 (s, 1H), 3.19 (d, J = 4.69 Hz, 4H), 3.01 (br s, 4H).

2-(6-(4-((6-Aminopyridin-3-yl)sulfonyl)piperazin-1-yl)-5-(1-methyl-1H-pyrazol-4-yl)pyridin-3-yl)-1,1,1,3,3,3-hexafluoropropan-2-ol (34). A solution of *tert*-butyl (5-((4-(3-chloro-5-(1,1,1,3,3,3-hexafluoro-2-hydroxypropan-2-yl)pyridin-2-yl)piperazin-1-yl)sulfonyl)pyridin-2-yl)carbamate (**19**) (0.500 g, 0.806 mmol), Pd(amphos)Cl$_2$ (0.057 g, 0.081 mmol), K$_2$CO$_3$ (0.446 g, 3.23 mmol), and 1-methyl-4-(4,4,5,5-tetramethyl-1,3,2-dioxaborolan-2-yl)-1H-pyrazole (0.336 g, 1.613 mmol) in 1,4-dioxane (8.0 mL)/H$_2$O (0.8 mL) was heated in a sealed tube at 140 °C for 1 h in the microwave. The solution was then filtered through a pad of Celite with MeOH, and the filtrate was concentrated. The residue was redissolved in DCM (20 mL) and TFA (10 mL) and stirred at room temperature for 30 min. The reaction was quenched with solid NaHCO$_3$ and diluted with H$_2$O and EtOAc. The organic layer was separated, dried over Na$_2$SO$_4$, filtered, and concentrated. The crude material was purified by column chromatography eluting with 0−7% (2 M NH$_3$ in MeOH) in DCM to give the title compound (0.170 g, 37%) as an off-white solid. MS (ESI pos. ion) m/z calcd for $C_{21}H_{21}F_6N_7O_3S$, 562; found, 563 (M + H). ^{1}H NMR (400 MHz, CD$_3$OD) δ 8.40−8.36 (m, 1H), 8.28 (d, J = 2.2 Hz, 1H), 7.97−7.92 (m, 1H), 7.83 (d, J = 2.0 Hz, 1H), 7.79−7.76 (m, 1H), 7.72 (dd, J = 2.5, 9.0 Hz, 1H), 6.64 (d, J = 9.0 Hz, 1H), 3.90 (s, 3H), 3.28−3.23 (m, 4H), 3.10−3.04 (m, 4H). Three exchangeable protons were not observed.

2-(6-(4-((6-Aminopyridin-3-yl)sulfonyl)piperazin-1-yl)-5-(1-ethyl-1H-pyrazol-4-yl)pyridin-3-yl)-1,1,1,3,3,3-hexafluoropropan-2-ol 2,2,2-trifluoroacetate (35). This material was prepared according to the procedure described for the synthesis of **33** using 1-ethyl-4-(4,4,5,5-tetramethyl-1,3,2-dioxaborolan-2-yl)-1H-pyrazole (0.067 g, 0.301 mmol). The TFA salt of the title compound was isolated (0.048 g, 46%) as a tan solid. MS (ESI pos. ion) m/z calcd for $C_{22}H_{23}F_6N_7O_3S$, 579; found, 580 (M + H). ^{1}H NMR (400 MHz, DMSO-d_6) δ 8.90−8.79 (m, 1H), 8.33 (s, 1H), 8.27 (d, J = 2.2 Hz, 1H), 8.14 (s, 1H), 7.78 (d, J = 2.0 Hz, 2H), 7.76−7.70 (m, 2H), 7.61−7.53 (dd, J = 2.5, 9.0 Hz, 1H), 6.74−6.63 (d, J = 9.0 Hz, 1H), 3.16 (d, J = 4.69 Hz, 4H), 3.01 (br s, 4H), 3.06−2.99 (m, 2H), 1.38−1.33 (m, 3H).

2-(6-(4-((6-Aminopyridin-3-yl)sulfonyl)piperazin-1-yl)-5-(1-iso-propyl-1H-pyrazol-4-yl)pyridin-3-yl)-1,1,1,3,3,3-hexafluoropropan-2-ol (36). This material was prepared according to the procedure described for the synthesis of **33** using 1-isopropyl-4-(4,4,5,5-tetramethyl-1,3,2-dioxaborolan-2-yl)-1H-pyrazole (0.071 g, 0.301 mmol). The TFA salt of the title compound was isolated (0.048 g, 45%) as a tan solid. MS (ESI pos. ion) m/z calcd for $C_{23}H_{25}F_6N_7O_3S$, 593; found, 594 (M + H). ^{1}H NMR (400 MHz, DMSO-d_6) δ 8.89−8.79 (m, 1H), 8.36−8.29 (m, 1H), 8.30−8.23 (d, J = 2.2 Hz, 1H), 8.17−8.10 (m, 1H), 7.83−7.75 (d, J = 2.0 Hz, 2H), 7.74−7.67 (m, 2H), 7.61−7.53 (dd, J = 2.5, 9.0 Hz, 1H), 6.70−6.62 (d, J = 9.0 Hz, 1H), 3.15 (d, J = 4.50 Hz, 4H), 3.01−2.96 (m, 4H), 2.85 (m, 1H), 1.41−1.39 (m, 6H).

2-(6-(4-((6-Aminopyridin-3-yl)sulfonyl)piperazin-1-yl)-5-(1-(tert-butyl)-1H-pyrazol-4-yl)pyridin-3-yl)-1,1,1,3,3,3-hexafluoropropan-2-ol (37). This material was prepared according to the procedure described for the synthesis of **33** using 1-(*tert*-butyl)-4-(4,4,5,5-tetramethyl-1,3,2-dioxaborolan-2-yl)-1H-pyrazole (0.075 g, 0.301 mmol). The TFA salt of the title compound was isolated (0.043 g, 39%) as a tan solid. MS (ESI pos. ion) m/z calcd for $C_{24}H_{27}F_6N_7O_3S$, 607; found, 608 (M + H). ^{1}H NMR (400 MHz, DMSO-d_6) δ 8.98−8.77 (m, 1H), 8.36−8.32 (m, 1H), 8.26−8.23 (d, J = 1.83 Hz, 1H), 8.11 (s, 1H), 7.84−7.81 (d, J = 2.0 Hz, 2H), 7.71−7.65 (dd, J = 2.5, 9.0 Hz, 2H), 7.60−7.57 (m, 1H), 6.73−6.54 (d, J = 9.0 Hz, 1H), 3.17 (br s, 4H), 2.99 (br s, 4H), 0.84 (dd, J = 2.74, 6.65 Hz, 9H).

2-(6-(4-((6-Aminopyridin-3-yl)sulfonyl)piperazin-1-yl)-5-(1,5-di-methyl-1H-pyrazol-4-yl)pyridin-3-yl)-1,1,1,3,3,3-hexafluoropropan-2-ol (38). This material was prepared according to the procedure described for the synthesis of **33** using 1,5-dimethyl-4-(4,4,5,5-tetramethyl-1,3,2-dioxaborolan-2-yl)-1H-pyrazole (0.067 g, 0.301 mmol). The TFA salt of the title compound was isolated (0.010 g, 10%) as a tan solid. MS (ESI pos. ion) m/z calcd for $C_{22}H_{23}F_6N_7O_3S$, 579; found, 580 (M + H). ^{1}H NMR (400 MHz, DMSO-d_6) δ 8.73−8.93 (m, 1H), 8.36 (s, 1H), 8.23 (d, J = 2.15 Hz, 1H), 8.15 (s, 1H), 7.97 (s, 1H), 7.76−7.61 (m, 1H), 7.52 (br s, 2H), 6.69−6.52 (m, 1H), 3.76 (s, 3H), 3.17 (d, J = 4.69 Hz, 4H), 2.87 (br s, 4H), 2.12 (s, 3H).

2-(6-(4-((6-Aminopyridin-3-yl)sulfonyl)piperazin-1-yl)-5-(1-methyl-3-(trifluoromethyl)-1H-pyrazol-4-yl)pyridin-3-yl)-1,1,1,3,3,3-hexafluoropropan-2-ol (39). This material was prepared according to the procedure described for the synthesis of **33** using 1-methyl-4-(4,4,5,5-tetramethyl-1,3,2-dioxaborolan-2-yl)-3-(trifluoromethyl)-1H-pyrazol (0.083 g, 0.301 mmol). The TFA salt of the title compound was isolated (0.059 g, 52%) as a tan solid. MS (ESI pos. ion) m/z calcd for $C_{22}H_{20}F_9N_7O_3S$, 633; found, 634 (M + H). ^{1}H NMR (400 MHz, DMSO-d_6) δ 9.00−8.78 (m, 1H), 8.44 (d, J = 2.35 Hz, 1H), 8.24 (d, J = 2.15 Hz, 1H), 8.15 (s, 1H), 7.97 (s, 1H), 7.70 (dd, J = 2.35, 9.00 Hz, 1H), 7.60 (d, J = 1.76 Hz, 1H), 6.65 (d, J = 9.00 Hz, 1H), 3.96 (s, 1H), 3.93 (s, 3H), 3.24−3.10 (m, 4H), 2.88 (br s, 4H).

2-(6-(4-((6-Aminopyridin-3-yl)sulfonyl)piperazin-1-yl)-5-(furan-3-yl)pyridin-3-yl)-1,1,1,3,3,3-hexafluoropropan-2-ol (40). This material was prepared according to the procedure described for the synthesis of **33** using furan-3-ylboronic acid (0.051 g, 0.452 mmol). The TFA salt of the title compound was isolated (0.024 g, 19%) as a tan solid. MS (ESI pos. ion) m/z calcd for $C_{21}H_{19}F_6N_5O_4S$, 551; found, 552 (M + H). ^{1}H NMR (400 MHz, DMSO-d_6) δ 8.98−8.81 (m, 1H), 8.39 (d, J = 1.96 Hz, 1H), 8.23 (d, J = 2.35 Hz, 1H), 8.10 (s, 1H), 7.77 (s, 2H), 7.705−7.55 (m, 1H), 7.01 (s, 2H), 6.82 (d, J = 0.78 Hz, 1H), 6.55 (d, J = 9.00 Hz, 1H), 3.21 (d, J = 4.69 Hz, 4H), 3.05−2.91 (m, 4H).

2-(6-(4-((6-Aminopyridin-3-yl)sulfonyl)piperazin-1-yl)-5-(4-methylthiophen-2-yl)pyridin-3-yl)-1,1,1,3,3,3-hexafluoropropan-2-ol (41). This material was prepared according to the procedure described for the synthesis of **34** from **19** (0.200 g, 0.323 mmol) using (4-methylthiophen-2-yl)boronic acid (0.092 g, 0.645 mmol). The title compound **41** was isolated (0.025 g, 13%) as an off-white solid. MS (ESI pos. ion) m/z calcd for $C_{22}H_{21}F_6N_5O_3S_2$, 581; found, 582 (M + H). ^{1}H NMR (400 MHz, CD$_3$OD) δ 8.43−8.39 (m, 1H), 8.28 (d, J = 2.2 Hz, 1H), 7.90−7.85 (m, 1H), 7.72 (dd, J = 2.4, 8.9 Hz, 1H), 7.18−7.12 (m, 1H), 7.07−7.01 (m, 1H), 6.65 (d, J = 8.8 Hz, 1H), 3.29−3.23 (m, 4H), 3.10−3.03 (m, 4H), 2.24 (s, 3H). Three exchangeable protons were not observed.

2-(6-(4-((6-Aminopyridin-3-yl)sulfonyl)piperazin-1-yl)-5-phenyl-pyridin-3-yl)-1,1,1,3,3,3-hexafluoropropan-2-ol (42). This material

was prepared according to the procedure described for the synthesis of **34** from **19** (0.060 g, 0.097 mmol) using phenyl boronic acid (0.018 g, 0.145 mmol). The title compound **42** was isolated (0.047 g, 86% yield) as a white solid. MS (ESI pos. ion) m/z calcd for $C_{23}H_{21}F_6N_5O_3S$, 561; found, 562 (M + H). ^{1}H NMR (400 MHz, DMSO-d_6) δ 8.85 (s, 1H), 8.42 (s, 1H), 8.21 (d, J = 2.35 Hz, 1H), 7.71−7.59 (m, 2H), 7.55−7.47 (m, 2H), 7.47−7.36 (m, 3H), 7.16 (br s, 2H), 6.60 (d, J = 8.80 Hz, 1H), 3.17 (d, J = 4.69 Hz, 4H), 2.85 (br s, 4H).

2-(6-(4-((6-Aminopyridin-3-yl)sulfonyl)piperazin-1-yl)-5-(2-fluorophenyl)pyridin-3-yl)-1,1,1,3,3,3-hexafluoropropan-2-ol (43).
Following a similar procedure as described previously in the synthesis of **33**, *tert*-butyl (5-((4-(3-bromo-5-(1,1,1,3,3,3-hexafluoro-2-hydroxypropan-2-yl)pyridin-2-yl)piperazin-1-yl)sulfonyl)pyridin-2-yl)-carbamate **20** (0.100 g, 0.151 mmol), and (2-fluorophenyl)boronic acid (0.063 g, 0.452 mmol) were used. The crude material was purified (Xbridge 19 × 100 mm, 10 μm Column, 40 mL/min flow rate, 0.1% NH_4OH in H_2O/MeCN) to give the title compound (0.038 g, 29%) as a light-yellow solid. MS (ESI pos. ion) m/z calcd for $C_{23}H_{20}F_7N_5O_3S$, 579; found, 580 (M + H). ^{1}H NMR (400 MHz, DMSO-d_6) δ 8.87 (s, 1H), 8.46 (d, J = 2.15 Hz, 1H), 8.18 (d, J = 2.35 Hz, 1H), 7.67 (s, 1H), 7.59 (dd, J = 2.54, 8.80 Hz, 1H), 7.49 (d, J = 7.82 Hz, 2H), 7.28 (d, J = 8.02 Hz, 2H), 7.03 (s, 2H), 6.55 (d, J = 8.80 Hz, 1H), 3.19 (d, J = 5.09 Hz, 4H), 2.85−2.72 (m, 4H).

2-(6-(4-((6-Aminopyridin-3-yl)sulfonyl)piperazin-1-yl)-5-(3-fluorophenyl)pyridin-3-yl)-1,1,1,3,3,3-hexafluoropropan-2-ol (44).
This material was prepared according to the procedure described for the synthesis of **43** from **20** using (3-fluorophenyl)boronic acid (0.063 g, 0.452 mmol). The title compound **44** was isolated (0.027 g, 26%) as a light-yellow solid. MS (ESI pos. ion) m/z calcd for $C_{23}H_{20}F_7N_5O_3S$, 579; found, 580 (M + H). ^{1}H NMR (400 MHz, DMSO-d_6) δ 8.99−8.72 (m, 1H), 8.44 (d, J = 2.15 Hz, 1H), 8.20 (d, J = 2.35 Hz, 1H), 7.75−7.65 (m, 1H), 7.59 (d, J = 2.54 Hz, 2H), 7.55−7.41 (d, J = 7.82 Hz, 1H), 7.36 (s, 2H), 7.28−7.18 (m, 1H), 7.02 (s, 1H), 6.55 (d, J = 9.00 Hz, 1H), 3.19 (br s, 4H), 2.85 (br s, 4H).

2-(6-(4-((6-Aminopyridin-3-yl)sulfonyl)piperazin-1-yl)-5-(4-fluorophenyl)pyridin-3-yl)-1,1,1,3,3,3-hexafluoropropan-2-ol (45).
This material was prepared according to the procedure described for the synthesis of **43** from **20** using (4-fluorophenyl)boronic acid (0.063 g, 0.452 mmol). The title compound **45** was isolated (0.035 g, 26%) as a light-yellow solid. MS (ESI pos. ion) m/z calcd for $C_{23}H_{20}F_7N_5O_3S$, 579; found, 580 (M + H). ^{1}H NMR (400 MHz, DMSO-d_6) δ 8.94−8.79 (m, 1H), 8.42 (d, J = 1.96 Hz, 1H), 8.20 (d, J = 2.54 Hz, 1H), 7.56 (d, J = 3.13 Hz, 4H), 7.25 (s, 2H), 7.02 (s, 2H), 6.54 (d, J = 8.80 Hz, 1H), 3.16 (br s, 4H), 2.85 (d, J = 4.11 Hz, 4H).

2-(2-(4-((6-Aminopyridin-3-yl)sulfonyl)piperazin-1-yl)-5-(1,1,1,3,3,3-hexafluoro-2-hydroxypropan-2-yl)pyridin-3-yl)phenol (46).
This material was prepared according to the procedure described for the synthesis of **43** from **20** using 2-hydroxyphenylboronic acid pinacol ester (0.066 g, 0.301 mmol). The crude product was adsorbed onto silica gel and chromatographed through a Redi-Sep prepacked silica gel column (40 g), eluting with a gradient of 0−20% 2 M NH_3·MeOH in DCM, to provide the title compound (0.056 g, 64%) as a tan solid. MS (ESI pos. ion) m/z calcd for $C_{23}H_{21}F_6N_5O_4S$, 577; found, 578 (M + H). ^{1}H NMR (400 MHz, DMSO-d_6) δ 9.61−9.54 (m, 1H), 9.22−9.13 (m, 1H), 8.79−8.72 (m, 1H), 8.41−8.33 (d, J = 4.50 Hz, 1H), 8.22−8.12 (ddd, J = 1.66, 7.58, 9.73 Hz, 1H), 7.71−7.62 (m, 1H), 7.62−7.53 (dd, J = 2.45, 8.90 Hz, 1H), 7.23−7.08 (m, 1H), 7.08−7.00 (m, 1H), 6.95−6.86 (m, 1H), 6.86−6.74 (m, 1H), 6.56−6.48 (d, J = 8.80 Hz, 1H), 5.80−5.69 (m, 1H), 3.20 (br s, 4H), 2.77 (br s, 4H).

N-(3-(2-(4-((6-Aminopyridin-3-yl)sulfonyl)piperazin-1-yl)-5-(1,1,1,3,3,3-hexafluoro-2-hydroxypropan-2-yl)pyridin-3-yl)phenyl)-methanesulfonamide (47). To a mixture of **23** (0.050 g, 0.096 mmol), 3-(methylsulfonylamino)phenylboronic acid (0.031 g, 0.144 mmol), 1,1-bis[(di-*tert*-butyl-*p*-methylaminophenyl]palladium(II) chloride (6.81 mg, 0.0096 mmol), and potassium carbonate (53.2 mg, 0.385 mmol) was added 1,4-dioxane (3 mL)/water (0.30 mL). The vial was sealed and heated at 140 °C for 45 min. The mixture was allowed to cool to room temperature, concentrated on silica gel, and purifed by chromatography through a Redi-Sep prepacked silica gel column (40 g), eluting with a gradient of 0−7% 2 M NH_3·MeOH in DCM, to provide

the title compound isolated (0.005 g, 8%) as a white solid. MS (ESI pos. ion) m/z calcd for $C_{24}H_{24}F_6N_6O_5S_2$, 654; found, 655 (M + H). ^{1}H NMR (400 MHz, CD$_3$OD) δ 8.49−8.43 (m, 1H), 8.23 (d, J = 2.2 Hz, 1H), 7.76−7.72 (m, 1H), 7.66 (dd, J = 2.5, 9.0 Hz, 1H), 7.45−7.39 (m, 2H), 7.25−7.20 (m, 2H), 6.64 (d, J = 9.0 Hz, 1H), 3.26−3.19 (m, 4H), 3.01−2.95 (m, 4H), 2.93 (s, 3H). Four exchangeable protons were not observed.

3-(2-(4-((6-Aminopyridin-3-yl)sulfonyl)piperazin-1-yl)-5-(1,1,1,3,3,3-hexafluoro-2-hydroxypropan-2-yl)pyridin-3-yl)-benzamide (48). This material was prepared according to the procedure described for the synthesis of **47** from **23** (0.050 g, 0.096 mmol) using (3-carbamoylphenyl)boronic acid (0.024 g, 0.144 mmol), and the mixture was heated in a sealed tube at 120 °C overnight. The product was purified by column chromatography twice eluting with 0−10% MeOH in DCM. This was followed by recryallization from EtOAc and hexanes. A final purification by column chromatography eluting with 0−100% EtOAc in hexanes followed by 0−7% MeOH in CH_2Cl_2 over 30 min gave the title compound (0.002 g, 4%) as an amorphous white solid. MS (ESI pos. ion) m/z calcd for $C_{24}H_{22}F_6N_6O_4S$, 604; found, 605 (M + H). ^{1}H NMR (400 MHz, CD$_3$OD) δ 8.49−8.45 (m, 1H), 8.22 (d, J = 2.2 Hz, 1H), 8.04−8.00 (m, 1H), 7.89−7.86 (m, 1H), 7.80−7.78 (m, 1H), 7.69−7.62 (m, 2H), 7.55−7.49 (m, 1H), 6.63 (d, J = 9.0 Hz, 1H), 3.24−3.19 (m, 4H), 2.94−2.88 (m, 4H). Five exchangeable protons were not observed.

2-(6-(4-((6-Aminopyridin-3-yl)sulfonyl)piperazin-1-yl)-5-(4-(methylsulfonyl)phenyl)pyridin-3-yl)-1,1,1,3,3,3-hexafluoropropan-2-ol (49). This material was prepared according to the procedure described for the synthesis of **48** from **23** (0.050 g, 0.096 mmol) using 4-(methanesulfonyl)benzeneboronic acid (0.029 g, 0.144 mmol). The crude material was purified by column chromatography, eluting with 0−7% MeOH in DCM, followed by recrystallization from Et$_2$O and hexanes. The title compound was isolated (10 mg, 16%) as a white solid. MS (ESI pos. ion) m/z calcd for $C_{24}H_{23}F_6N_5O_5S_2$, 639; found, 640 (M + H). ^{1}H NMR (400 MHz, CD$_3$OD) δ 8.51−8.48 (m, 1H), 8.25−8.22 (m, 1H), 8.01−7.97 (m, 2H), 7.80−7.75 (m, 3H), 7.66 (dd, J = 2.4, 8.9 Hz, 1H), 6.64 (d, J = 8.8 Hz, 1H), 3.26−3.22 (m, 4H), 3.17 (s, 3H), 2.97−2.91 (m, 4H). Three exchangeable protons were not observed.

2-(2-(4-((6-Aminopyridin-3-yl)sulfonyl)piperazin-1-yl)-[3,4'-bipyridin]-5-yl)-1,1,1,3,3,3-hexafluoropropan-2-ol (50). This material was prepared according to the procedure described for the synthesis of **34** from **19** (0.158 g, 0.255 mmol) using pyridin-4-ylboronic acid (0.063 g, 0.510 mmol). The crude material was purified by preparative TLC eluting with 10% 2 M MH$_3$/MeOH in DCM, to give the desired product (0.026 g, 20%) as a tan solid. MS (ESI pos. ion) m/z calcd for $C_{23}H_{20}F_6N_6O_3S$, 562; found, 563 (M + H). ^{1}H NMR (400 MHz, DMSO-d_6) δ 8.94 (br s, 1H), 8.62 (d, J = 2.15 Hz, 2H), 8.46 (d, J = 1.96 Hz, 1H), 8.19 (d, J = 2.15 Hz, 1H), 7.71 (br s, 1H), 7.66−7.42 (m, 3H), 7.05 (br s, 2H), 6.54 (d, J = 8.41 Hz, 1H), 3.19 (br s, 4H), 2.85 (br s, 4H).

2-(2-(4-((6-Aminopyridin-3-yl)sulfonyl)piperazin-1-yl)-[3,3'-bipyridin]-5-yl)-1,1,1,3,3,3-hexafluoropropan-2-ol (51). This material was prepared according to the procedure described for the synthesis of **34** from **19** (0.892 g, 1.439 mmol) using 3-pyridylboronic acid (0.708 g, 5.760 mmol). The title compound was isolated (0.577 g, 71%) as a pale-yellow solid. MS (ESI pos. ion) m/z calcd for $C_{22}H_{20}F_6N_6O_3S$, 562; found, 563 (M + H). ^{1}H NMR (400 MHz, DMSO-d_6) δ 8.91 (s, 1H), 8.72 (d, J = 1.56 Hz, 1H), 8.58 (d, J = 3.33 Hz, 1H), 8.45 (s, 1H), 8.17 (d, J = 2.35 Hz, 1H), 7.94 (d, J = 7.63 Hz, 1H), 7.68 (s, 1H), 7.58 (dd, J = 2.35, 8.80 Hz, 1H), 7.44 (dd, J = 4.69, 7.82 Hz, 1H), 7.04 (s, 2H), 6.52 (d, J = 8.80 Hz, 1H), 3.15 (br s, 4H), 2.81 (br s, 4H).

2-(2-(4-((6-Aminopyridin-3-yl)sulfonyl)piperazin-1-yl)-4'-fluoro-[3,3'-bipyridin]-5-yl)-1,1,1,3,3,3-hexafluoropropan-2-ol (52). This material was prepared according to the procedure described for the synthesis of **43** from **20** (0.100 g, 0.151 mmol) using (4-fluoropyridin-3-yl)boronic acid (0.064 g, 0.452 mmol). The title compound was isolated (0.07 g, 6%) as a tan solid. MS (ESI pos. ion) m/z calcd for $C_{22}H_{19}F_7N_6O_3S$, 580; found, 581 (M + H). ^{1}H NMR (400 MHz, DMSO-d_6) δ 9.00−8.85 (m, 1H), 8.75−8.69 (m, 1H), 8.68−8.61 (d, J = 2.15 Hz,1H), 8.54−8.48 (d, J = 2.15 Hz, 1H), 8.20−8.14 (d, J = 2.35 Hz, 1H), 7.79−7.72 (m, 1H), 7.61−7.54 (dd, J = 2.45, 8.90 Hz, 1H), 7.48−

7.37 (m, 1H), 7.06−6.99 (m, 2H), 6.60−6.40 (d, J = 8.80 Hz, 1H), 3.28−3.10 (m, 4H), 2.86−2.73 (m, 4H).

2-(2-(4-((6-Aminopyridin-3-yl)sulfonyl)piperazin-1-yl)-5′-fluoro-[3,3′-bipyridin]-5-yl)-1,1,1,3,3,3-hexafluoropropan-2-ol (53). This material was prepared according to the procedure described for the synthesis of **43** from **20** (0.100 g, 0.151 mmol) using (5-fluoropyridin-3-yl)boronic acid (0.064 g, 0.452 mmol). The title compound was isolated (0.034 g, 26%) as a tan solid. MS (ESI pos. ion) m/z calcd for $C_{22}H_{19}F_7N_6O_3S$, 580; found, 581 (M + H). ^{1}H NMR (400 MHz, DMSO-d_6) δ 9.00−8.82 (m, 1H), 8.69−8.54 (m, 2H), 8.49 (d, J = 2.15 Hz, 1H), 8.20 (d, J = 2.35 Hz, 1H), 8.00−7.90 (m, 1H), 7.83−7.68 (m, 1H), 7.60 (dd, J = 2.54, 8.80 Hz, 1H), 7.02 (s, 2H), 6.55 (d, J = 8.80 Hz, 1H), 3.18 (br s, 4H), 2.85 (d, J = 4.30 Hz, 4H).

2-(2-(4-((6-Aminopyridin-3-yl)sulfonyl)piperazin-1-yl)-5′-methyl-[3,3′-bipyridin]-5-yl)-1,1,1,3,3,3-hexafluoropropan-2-ol (54). This material was prepared according to the procedure described for the synthesis of **33** from **20** (0.100 g, 0.151 mmol) using (5-methylpyridin-3-yl)boronic acid (0.041 g, 0.301 mmol). The TFA salt of the title compound was isolated (0.019 g, 19%) as a tan solid. MS (ESI pos. ion) m/z calcd for $C_{23}H_{22}F_6N_6O_3S$, 576; found, 577 (M + H). ^{1}H NMR (400 MHz, DMSO-d_6) δ 8.98−8.78 (m, 1H), 8.58 (d, J = 2.15 Hz, 1H), 8.45 (d, J = 1.96 Hz, 1H), 8.20 (d, J = 2.35 Hz, 1H), 7.89−7.82 (m, 1H), 7.64−7.70 (m, 1H), 7.63−7.56 (m, 1H), 7.37−7.22 (m, 1H), 7.02 (s, 2H), 6.55 (d, J = 8.61 Hz, 1H), 3.19 (d, J = 4.69 Hz, 4H), 2.86 (br s, 4H), 2.31 (br s, 3H).

2-(2-(4-((6-Aminopyridin-3-yl)sulfonyl)piperazin-1-yl)-6′-methyl-[3,3′-bipyridin]-5-yl)-1,1,1,3,3,3-hexafluoropropan-2-ol (55). This material was prepared according to the procedure described for the synthesis of **43** from **20** (0.100 g, 0.151 mmol) using (6-methylpyridin-3-yl)boronic acid (0.062 g, 0.452 mmol). The title compound was isolated (0.017 g, 13%) as a tan solid. MS (ESI pos. ion) m/z calcd for $C_{23}H_{22}F_6N_6O_3S$, 576; found, 577 (M + H). ^{1}H NMR (400 MHz, DMSO-d_6) δ 8.98−8.78 (m, 1H), 8.58 (d, J = 2.15 Hz, 1H), 8.45 (d, J = 1.96 Hz, 1H), 8.20 (d, J = 2.35 Hz, 1H), 7.89−7.82 (m, 1H), 7.70−7.64 (m, 1H), 7.63−7.56 (m, 1H), 7.37−7.22 (m, 1H), 7.02 (s, 2H), 6.55 (d, J = 8.61 Hz, 1H), 3.19 (d, J = 4.69 Hz, 4H), 2.86 (br s, 4H), 2.46 (br s, 3H).

2-(2-(4-((6-Aminopyridin-3-yl)sulfonyl)piperazin-1-yl)-6′-methoxy-[3,3′-bipyridin]-5-yl)-1,1,1,3,3,3-hexafluoropropan-2-ol (56). This material was prepared according to the procedure described for the synthesis of **43** from **20** (0.100 g, 0.151 mmol) using (6-methoxypyridin-3-yl)boronic acid (0.069 g, 0.52 mmol). The title compound was isolated (0.008 g, 6%) as a tan solid. MS (ESI pos. ion) m/z calcd for $C_{23}H_{22}F_6N_6O_4S$, 592; found, 593 (M + H). ^{1}H NMR (400 MHz, DMSO-d_6) δ 8.91−8.82 (m, 1H), 8.49−8.36 (d, J = 2.15 Hz, 1H), 8.32−8.27 (d, J = 1.96 Hz, 1H), 8.22−8.17 (d, J = 2.35 Hz, 1H), 7.91−7.84 (m, 1H), 7.68−7.63 (m, 1H), 7.63−7.57 (m, 1H), 7.05−6.99 (m, 2H), 6.88−6.82 (m, 1H), 6.60−6.46 (d, J = 8.61 Hz, 1H), 3.89 (s, 3H), 3.18 (d, J = 5.28 Hz, 4H), 2.90−2.76 (m, 4H).

2-(2-(4-((6-Aminopyridin-3-yl)sulfonyl)piperazin-1-yl)-5′-methoxy-[3,3′-bipyridin]-5-yl)-1,1,1,3,3,3-hexafluoropropan-2-ol (57). This material was prepared according to the procedure described for the synthesis of **43** from **20** (0.100 g, 0.151 mmol) using (5-methoxypyridin-3-yl)boronic acid (0.069 g, 0.452 mmol). The title compound was isolated (0.029 g, 22%) as a tan solid. MS (ESI pos. ion) m/z calcd for $C_{23}H_{22}F_6N_6O_4S$, 592; found, 593 (M + H). ^{1}H NMR (400 MHz, DMSO-d_6) δ 8.95−8.83 (m, 1H), 8.52−8.40 (d, J = 2.15 Hz, 1H), 8.20 (d, J = 1.96 Hz, 2H), 7.79−7.68 (d, J = 2.35 Hz, 1H), 7.64−7.51 (m, 1H), 7.15−7.10 (m, 1H), 7.03 (s, 2H), 6.94 (d, J = 8.61 Hz, 1H), 6.62−6.50 (m, 1H), 3.88 (s, 3H), 3.21 (br s, 4H), 2.86 (d, J = 4.11 Hz, 4H).

2-(6-(4-((6-Aminopyridin-3-yl)sulfonyl)piperazin-1-yl)-5-(benzo-[b]thiophen-5-yl)pyridin-3-yl)-1,1,1,3,3,3-hexafluoropropan-2-ol (58). This material was prepared according to the procedure described for the synthesis of **34** from **19** (0.100 g, 0.192 mmol) using 2-(benzo[b]thiophen-5-yl)-4,4,5,5-tetramethyl-1,3,2-dioxaborolane (0.100 g, 0.385 mmol). The title compound was isolated (0.009 g, 8%) as a tan solid. MS (ESI pos. ion) m/z calcd for $C_{25}H_{21}F_6N_5O_3S_2$, 617; found, 618 (M + H). ^{1}H NMR (400 MHz, DMSO-d_6) δ 8.42 (s, 1H), 8.15 (d, J = 2.23 Hz, 1H), 8.08−7.97 (m, 2H), 7.83 (d, J = 5.21 Hz, 1H),

7.73 (br s, 1H), 7.66−7.46 (m, 2H), 7.39 (br s, 1H), 7.02 (s, 2H), 6.53 (d, J = 8.82 Hz, 1H), 5.74 (s, 1H), 3.17 (s, 4H), 2.80 (br s, 4H).

2-(6-(4-((6-Aminopyridin-3-yl)sulfonyl)piperazin-1-yl)-5-(benzo-[d]thiazol-5-yl)pyridin-3-yl)-1,1,1,3,3,3-hexafluoropropan-2-ol (59). This material was prepared according to the procedure described for the synthesis of **34** from **19** (0.100 g, 0.192 mmol) using 5-(4,4,5,5-tetramethyl-1,3,2-dioxaborolan-2-yl)benzo[d]thiazole (0.100 g, 0.385 mmol). The title compound was isolated (0.009 g, 8%) as a light-yellow solid. MS (ESI pos. ion) m/z calcd for $C_{24}H_{20}F_6N_6O_3S_2$, 618; found, 619 (M + H). ^{1}H NMR (400 MHz, DMSO-d_6) δ 9.45 (s, 1H), 8.44 (s, 1H), 8.31−8.18 (m, 3H), 7.76 (br s, 1H), 7.64 (d, J = 8.08 Hz, 1H), 7.55 (dd, J = 8.85 Hz, 1H), 7.00 (s, 2H), 6.52 (d, J = 8.88 Hz, 1H), 5.75 (s, 1H), 3.18 (br s, 4H), 2.82 (br s, 4H).

2-(6-(4-((6-aminopyridin-3-yl)sulfonyl)piperazin-1-yl)-5-(benzo-[d]oxazol-5-yl)pyridin-3-yl)-1,1,1,3,3,3-hexafluoropropan-2-ol (60). This material was prepared according to the procedure described for the synthesis of **34** from **19** (0.100 g, 0.192 mmol) using 5-(4,4,5,5-tetramethyl-1,3,2-dioxaborolan-2-yl)benzo[d]oxazole (0.094 g, 0.385 mmol). The title compound was isolated (0.008 g, 6%) as a tan solid. MS (ESI pos. ion) m/z calcd for $C_{24}H_{20}F_6N_6O_4S$, 602; found, 603 (M + H). ^{1}H NMR (400 MHz, DMSO-d_6) δ 8.92−8.70 (m, 1H), 8.27−8.10 (d, J = 2.35 Hz, 1H), 7.83−7.63 (dd, J = 2.35, 8.80 Hz, 2H), 7.65−7.51 (m, 2H), 7.09−6.92 (d, J = 5.10 Hz, 1H), 6.84−6.71 (m, 1H), 6.59−6.45 (d, J = 8.61 Hz, 2H), 3.74−3.55 (m, 2H), 3.26−3.06 (m, 4H), 2.96 (s, 4H).

2-(6-(4-((6-Aminopyridin-3-yl)sulfonyl)piperazin-1-yl)-5-(2-methylbenzo[d]oxazol-5-yl)pyridin-3-yl)-1,1,1,3,3,3-hexafluoropropan-2-ol (61). This material was prepared according to the procedure described for the synthesis of **34** from **19** (0.100 g, 0.192 mmol) using 2-methyl-5-(4,4,5,5-tetramethyl-1,3,2-dioxaborolan-2-yl)benzo[d]-oxazole (0.069 g, 0.385 mmol). The title compound was isolated (0.012 g, 12%) as a light-yellow solid. MS (ESI pos. ion) m/z calcd for $C_{25}H_{22}F_6N_6O_4S$, 616; found, 617 (M + H). ^{1}H NMR (400 MHz, DMSO-d_6) δ 8.96−8.70 (m, 1H), 8.47−8.34 (m, 1H), 8.22−8.09 (m, 1H), 7.78−7.71 (m, 1H), 7.71−7.63 (m, 2H), 7.59−7.52 (m, 2H), 7.52−7.37 (m, 1H), 7.00 (s, 1H), 6.85−6.68 (m, 1H), 6.59−6.46 (m, 1H), 3.22−3.05 (m, 4H), 2.96 (s, 3H), 2.80 (br s, 3H).

5-(2-(4-((6-Aminopyridin-3-yl)sulfonyl)piperazin-1-yl)-5-(1,1,1,3,3,3-hexafluoro-2-hydroxypropan-2-yl)pyridin-3-yl)-1-methylindolin-2-one (62). This material was prepared according to the procedure described for the synthesis of **48** from **23** (0.100 g, 0.192 mmol) using 1-methyl-5-(4,4,5,5-tetramethyl-1,3,2-dioxaborolan-2-yl)-indolin-2-one (0.106 g, 0.385 mmol). The title compound was isolated (0.009 g, 7%) as a tan solid. MS (ESI pos. ion) m/z calcd for $C_{26}H_{24}F_6N_6O_4S$, 630; found, 631 (M + H). ^{1}H NMR (400 MHz, DMSO-d_6) δ 8.91−8.661 (m, 1H), 8.36 (s, 1H), 8.28−8.19 (d, J = 2.35 Hz, 1H), 7.71−7.57 (dd, J = 2.35, 8.80 Hz, 2H), 7.57−7.47 (br, s, 1H), 7.47−7.34 (m, 1H), 7.12−6.92 (d, J = 5.10 Hz, 1H), 6.93−6.80 (m, 1H), 6.59−6.49 (d, J = 8.76 Hz, 1H), 3.74−3.55 (m, 1H), 3.43 (s, 1H), 3.17 (m, 7H), 3.02−2.94 (m, 1H), 2.84 (d, J = 3.33 Hz, 4H).

5-(2-(4-((6-Aminopyridin-3-yl)sulfonyl)piperazin-1-yl)-5-(1,1,1,3,3,3-hexafluoro-2-hydroxypropan-2-yl)pyridin-3-yl)indolin-2-one (63). This material was prepared according to the procedure described for the synthesis of **34** from **19** (0.100 g, 0.192 mmol) using 5-(4,4,5,5-tetramethyl-1,3,2-dioxaborolan-2-yl)indolin-2-one (0.100 g, 0.385 mmol). The title compound was isolated (0.015 g, 13%) as a white solid. MS (ESI pos. ion) m/z calcd for $C_{25}H_{22}F_6N_6O_4S$, 616; found, 617 (M + H). ^{1}H NMR (400 MHz, DMSO-d_6) δ 10.48 (s, 1H), 8.91−8.66 (m, 1H), 8.36 (s, 1H), 8.20 (d, J = 2.35 Hz, 1H), 7.62 (dd, J = 2.35, 8.80 Hz, 2H), 7.35 (s, 1H), 7.06−6.92 (m, 2H), 6.93−6.80 (m, 1H), 6.53 (d, J = 8.61 Hz, 1H), 3.74−3.55 (m, 1H), 3.43 (s, 1H), 3.17 (br s, 4H), 3.02−2.94 (m, 1H), 2.84 (d, J = 3.33 Hz, 4H).

2-(6-(4-((6-Aminopyridin-3-yl)sulfonyl)piperazin-1-yl)-5-(1H-indazol-5-yl)pyridin-3-yl)-1,1,1,3,3,3-hexafluoropropan-2-ol (64). This material was prepared according to the procedure described for the synthesis of **33** from **20** (0.100 g, 0.151 mmol) using tetramethyl-1,3,2-dioxaborolane-2-yl)-1H-indazole (0.073 g, 0.301 mmol). The TFA salt of the title compound was isolated (0.013 g, 14%) as a tan solid. MS (ESI pos. ion) m/z calcd for $C_{24}H_{21}F_6N_7O_3S$, 601; found, 602 (M + H). ^{1}H NMR (400 MHz, DMSO-d_6) δ 8.98−8.71 (m, 1H), 8.41 (s, 2H), 8.20 (d, J = 2.15 Hz, 1H), 8.08 (s, 1H), 7.87 (s, 1H), 7.70 (s, 1H), 7.68−7.60

(m, 1H), 7.59−7.54 (m, 1H), 7.51 (d, J = 1.17 Hz, 1H), 6.62 (s, 1H), 3.16 (d, J = 4.69 Hz, 4H), 2.84 (br s, 4H), 1.15 (d, J = 13.30 Hz, 2H).

2-(6-(4-((6-Aminopyridin-3-yl)sulfonyl)piperazin-1-yl)-5-(1H-indazol-4-yl)pyridin-3-yl)-1,1,1,3,3,3-hexafluoropropan-2-ol (65). This material was prepared according to the procedure described for the synthesis of **48** from **23** (0.050 g, 0.096 mmol) using (1*H*-indazol-4-yl)boronic acid (0.023 g, 0.144 mmol). The crude product was purified by column chromatography eluting with 0−10% MeOH in DCM. This was followed by another purification by column chromatography eluting with 0−100% EtOAc in hexanes followed by another purification by column chromatography eluting with 0−7% MeOH in DCM to yield the title compound (0.002 g, 3%) as a white solid. MS (ESI pos. ion) *m/z* calcd for $C_{24}H_{21}F_6N_7O_3S$, 601; found, 602 (M + H). ^{1}H NMR (400 MHz, CD$_3$OD) δ 8.55−8.49 (m, 1H), 8.13 (d, J = 2.2 Hz, 1H), 7.91−7.87 (m, 1H), 7.79−7.75 (m, 1H), 7.60−7.54 (m, 2H), 7.49−7.42 (m, J = 7.0 Hz, 1H), 7.21 (d, J = 7.0 Hz, 1H), 6.60 (d, J = 9.0 Hz, 1H), 3.23−3.16 (m, 4H), 2.73−2.65 (m, 4H). Four exchangeable protons were not observed.

2-(6-(4-((6-Aminopyridin-3-yl)sulfonyl)piperazin-1-yl)-5-(1H-indol-2-yl)pyridin-3-yl)-1,1,1,3,3,3-hexafluoropropan-2-ol (66). This material was prepared according to the procedure described for the synthesis of **34** from **19** (0.100 g, 0.192 mmol) using 2-(4,5,5-tetramethyl-1,3,2-dioxaborolan-2-yl)-1*H*-indole (0.094 g, 0.385 mmol). The title compound was isolated (0.016 g, 14%) as a tan solid. MS (ESI pos. ion) *m/z* calcd for $C_{25}H_{22}F_6N_6O_3S$, 600; found, 601 (M + H). ^{1}H NMR (400 MHz, DMSO-d_6) δ 11.30 (br s, 1H), 8.40 (s,1H) 8.19 (d, J = 2.23 Hz, 1H), 7.94 (br s, 1H), 7.58 (dd, J = 8.91 Hz, 1H), 7.51 (d, J = 7.45 Hz, 1H), 7.39−7.26 (m, 1H), 7.13 (t, J = 7.45 Hz, 1H), 7.08−6.95 (m, 2H), 6.76 (d, J = 7.33 Hz, 1H), 6.69 (s, 1H), 6.57 (d, J = 8.99 Hz, 1H), 5.74 (s, 1H), 3.18 (br s, 4H), 3.06 (m, 4H).

2-(6-(4-((6-Aminopyridin-3-yl)sulfonyl)piperazin-1-yl)-5-(benzo[b]thiophen-2-yl)pyridin-3-yl)-1,1,1,3,3,3-hexafluoropropan-2-ol (67). This material was prepared according to the procedure described for the synthesis of **34** from **19** (0.100 g, 0.192 mmol) using benzo[*b*]thiophen-2-ylboronic acid (0.068 g, 0.385 mmol). The title compound was isolated (0.007 g, 7%) as a tan solid. MS (ESI pos. ion) *m/z* calcd for $C_{25}H_{21}F_6N_5O_3S_2$, 617; found, 618 (M + H). ^{1}H NMR (400 MHz, DMSO-d_6) δ 8.46 (s, 1H), 8.20 (d, J = 2.29 Hz, 1H), 7.97 (br s, 1H), 7.92 (d, J = 7.68 Hz, 1H), 7.82 (d, J = 7.33 Hz, 1H), 7.76 (s, 1H), 7.61 (d, J = 8.88 Hz, 1H), 7.48−7.28 (m, 2H), 7.04 (s, 1H), 6.55 (d, J = 8.88 Hz, 1H), 5.74 (s, 1H), 3.27 (s, 4H), 3.17 (br s, 1H), 2.98 (br s, 4H).

ASSOCIATED CONTENT

Supporting Information

Standard deviations for Tables 1−4; blood glucose measurements of postoral administration of compounds **51** and **1** (10, 30, 100, mg/kg) to *db/db* mice; unbound plasma concentrations of **51** from the efficacy study (Figure 7b) and the unbound plasma concentrations from the pharmacodynamic study (Figure 7d) plotted on the same graph; and calculation details for dihedral angle plot in Figure 4. This material is available free of charge via the Internet at http://pubs.acs.org. The cocrystal structure of hGKRP + compound **51** has been deposited in the Protein Data Bank with PDB code: 4OLH (see ref 7 for experimental details of crystallography).

AUTHOR INFORMATION

Corresponding Authors
*(F.-T.H.) Tel: 805-447-4992. E-mail: fhong@amgen.com.
*(M.H.N.) Tel: 805-447-1552. E-mail: markn@amgen.com.
Notes
The authors declare no competing financial interest.

ACKNOWLEDGMENTS

ABBREVIATIONS USED

GK, glucokinase; GKA, glucokinase activator; GKRP, glucokinase regulatory protein; RLM, rat liver microsomes; HLM, human liver microsomes; alpha, amplified luminescent proximity homogeneous assay; SFC, supercritical fluid chromatography; PK, pharmacokinetics; CL, clearance; MRT, mean residence time; AUC, area under curve; Vdss, volume of distribution; F, bioavailability; B/P, blood to plasma ratio; Fu, fraction unbound; IHC, immunohistochemistry; CYP, cytochrome P450; EC$_{50}$, half maximal effective concentration; IC$_{50}$, half maximal inhibitory concentration

REFERENCES

(1) Agius, L. Glucokinase and Molecular Aspects of Liver Glycogen Metabolism. *Biochem. J.* **2008**, *414*, 1−18.
(2) Matschinsky, F. M.; Liang, Y.; Kesavan, P.; Wang, L.; Froguel, P.; Velho, G.; Cohen, D.; Permutt, M. A.; Tanizawa, Y.; Jetton, T. L.; Niswender, K.; Magnuson, M. Glucokinase as Glucose Sensor and Metabolic Signal Generator in Pancreatic Beta-Cells and Hepatocytes. *Diabetes* **1990**, *39*, 647−652.
(3) Anderka, O.; Boyken, J.; Aschenbach, U.; Batzer, A.; Boscheinen, O.; Schmoll, D. Biophysical Characterization of the Interaction Between Hepatic Glucokinase and its Regulatory Protein: Impact of Physiological and Pharmacological Effectors. *J. Biol. Chem.* **2008**, *283*, 31333−31340.
(4) Vandercammen, A.; Van Schaftingen, E. The Mechanism by Which Rat Liver Glucokinase Is Inhibited by the Regulatory Protein. *Eur. J. Biochem.* **1990**, *191*, 483−489.
(5) Rees, M. G.; Gloyn, A. L. Small Molecular Glucokinase Activators: Has Another New Anti-Diabetic Therapeutic Lost Favour? *Br. J. Pharmacol.* **2013**, *168*, 335−338.
(6) (a) Pfefferkorn, J. A. Strategies for the Design of Hepatoselective Glucokinase Activators to Treat Type 2 Diabetes. *Expert Opin. Drug Discovery* **2013**, *8*, 319−330. (b) Pfefferkorn, J. A.; Guzman-Perez, A.; Litchfield, J.; Aiello, R.; Treadway, J. L.; Pettersen, J.; Minich, M. L.; Filipski, K. J.; Jones, C. S.; Tu, M.; Aspnes, G.; Risley, H.; Bian, J.; Stevens, B. D.; Bourassa, P.; D'Aquila, T.; Baker, L.; Barucci, N.; Robertson, A. S.; Bourbonais, F.; Derksen, D. R.; MacDougall, M.; Cabrera, O.; Chen, J.; Lapworth, A. L.; Landro, J. A.; Zavadoski, W. J.; Atkinson, K.; Haddish-Berhane, N.; Tan, B.; Yao, L.; Kosa, R. E.; Varma, M. V.; Feng, B.; Duignan, D. B.; El-Kattan, A.; Murdande, S.; Liu, S.; Ammirati, M.; Knafels, J.; DaSilva-Jardine, P.; Sweet, L.; Liras, S.; Rolph, T. P. Discovery of (*S*)-6-(3-Cyclopentyl-2-(4-(trifluoromethyl)-1*H*-imidazol-1-yl)propanamido)nicotinic Acid as a Hepatoselective Glucokinase Activator Clinical Candidate for Treating Type 2 Diabetes Mellitus. *J. Med. Chem.* **2012**, *55*, 1318−1333.
(7) Ashton, K.; Bartberger, M. D.; Bo, Y.; Bryan, M. C.; Croghan, M.; Fotsch, C. H.; Hale, C. H.; Kunz, R. K.; Liu, L.; Nishimura, N.; Norman, M. H.; Pennington, L. D.; Poon, S. F.; Stec, M. M.; St. Jean, D. J., Jr.; Tamayo, N. A.; Tegley, C. M.; Yang, K. Preparation of Sulfonylpiperazine Derivatives That Interact with Glucokinase Regulatory Protein for the Treatment of Diabetes and Other Diseases. PCT Int. Appl. WO 2012027261, 2012.
(8) Lloyd, D. J.; St. Jean, D. J., Jr.; Kurzeja, R. J. M.; Wahl, R. C.; Michelsen, K.; Cupples, R.; Chen, M.; Wu, J.; Sivits, G.; Helmering, J.; Ashton, K. S.; Pennington, L. D.; Fotsch, C. H.; Vazir, M.; Chen, K.; Chmait, S.; Zhang, J.; Liu, L.; Norman, M. H.; Andrews, K. A.; Bartberger, M. D.; Van, G.; Galbreath, E. J.; Vonderfecht, S. L.; Wang, M.; Jordan, S. R.; Véniant, M. M.; Hale, C. Anti-Diabetic Effects of a Glucokinase Regulatory Protein Small Molecule Disruptor. *Nature* **2013**, *504*, 437−440.
(9) Ashton, K. S.; Andrews, K. L.; Bryan, M. C.; Chen, J.; Chen, K.; Chen, M.; Chmait, S.; Croghan, M.; Cupples, R.; Fotsch, C.; Helmering, J.; Jordan, S. R.; Kurzeja, R. J. M.; Michelsen, K.; Pennington, L. D.;

Poon, S. F.; Sivits, G.; Van, G.; Vonderfecht, S. L.; Wahl, R. C.; Zhang, J.; Lloyd, D. J.; Hale, C.; St. Jean, D. J., Jr. Small Molecule Disruptors of the Glucokinase–Glucokinase Regulatory Protein Interaction: 1. Discovery of a Novel Tool Compound for in Vivo Proof-of-Concept. *J. Med. Chem.* **2014**, *57*, 309–324.

(10) St. Jean, D. J., Jr.; Ashton, K. S.; Bartberger, M. D.; Chen, J.; Chmait, S.; Cupples, R.; Galbreath, E.; Helmering, J.; Hong, F.-T.; Jordan, S. R.; Liu, L.; Kunz, R. K.; Michelsen, K.; Nishimura, N.; Pennington, L. D.; Poon, S. F.; Reid, D.; Sivits, G.; Stec, M. M.; Tadesse, S.; Tamayo, N.; Van, G.; Yang, K.; Zhang, J.; Norman, M. H.; Fotsch, C.; Lloyd, D. J.; Hale, C. Small Molecule Disruptors of the Glucokinase–Glucokinase Regulatory Protein Interaction: 2. Leveraging Structure-Based Drug Design to Identify Analogs with Improved Pharmacokinetic Profiles. *J. Med. Chem.* **2014**, *57*, 325–338.

(11) Nishimura, N.; Norman, M. H.; Liu, L.; Yang, K.; Ashton, K. S.; Bartberger, M. D.; Chen, J.; Chmait, S.; Cupples, R.; Fotsch, C.; Helmering, J.; Jordan, S. R.; Kunz, R. K.; Poon, S. F.; Siegmund, A.; Sivits, G.; Lloyd, D. J.; Hale, C.; St. Jean, D. J., Jr. Small Molecule Disruptors of the Glucokinase–Glucokinase Regulatory Protein Interaction: 3. Structure–Activity Relationships within the Aryl Carbinol Region of the *N*-Arylsulfonamido-*N*′-aryl-piperazine Series. *J. Med. Chem.* **2014**, *57*, 3094–3116.

(12) For detailed methods of obtaining GKRP crystals and data analysis, see ref 7.

(13) Pautsch, A.; Stadler, N.; Lohle, A.; Rist, W.; Berg, A.; Glocker, L.; Nar, H.; Reinert, D.; Lenter, M.; Heckel, A.; Schnapp, G.; Kauschke, S. G. Crystal Structure of Glucokinase Regulatory Protein. *Biochemistry* **2013**, *52*, 3523–3531.

(14) See Supporting Information for details of calculations and data analysis of this quantum mechanical study.

(15) This two-step sequence has been utilized to prepare structurally similar intermediates, see ref 6.

(16) Ashton, K.; Bourbeau, M. P.; Hong, F.-T.; Liu, L.; Nishimura, N.; Norman, M. H.; Poon, S. F.; Stec, M. M.; St. Jean, D. J., Jr.; Tamayo, N. A.; Yang, K. C. Preparation of Cyclic Sulfonyl Compounds That Interact with Glucokinase Regulatory Protein for Use in Treating Type 2 Diabetes and Other Diseases. PCT Int. Appl. WO 2013123444, 2013.

(17) Biscoe, M. R.; Fors, B. P.; Buchwald, S. L. A New Class of Easily Activated Palladium Precatalysts for Facile C–N Cross-Coupling Reactions and the Low Temperature Oxidative Addition of Aryl Chlorides. *J. Am. Chem. Soc.* **2008**, *130*, 6686–6687.

(18) Buxaderas, E.; Alonso, D. A.; Najera, C. Copper-Free Oxime-Palladacycle-Catalyzed Sonogashira Alkynylation of Deactivated Aryl Bromides and Chlorides in Water under Microwave Irradiation. *Eur. J. Org. Chem.* **2013**, *26*, 5864–5870.

(19) Guram, A. S.; Wang, X.; Bunel, E. E.; Faul, M. M.; Larsen, R. D.; Martinelli, M. J. New Catalysts for Suzuki–Miyaura Coupling Reactions of Heteroatom-Substituted Heteroaryl Chlorides. *J. Org. Chem.* **2007**, *72*, 5104–5112.

(20) Wang, X.; Zhi, B.; Baum, J.; Chen, Y.; Crockett, R.; Huang, L.; Eisenberg, S.; Ng, J.; Larsen, R.; Martinelli, M.; Reider, P. A Practical Synthesis of 2-((1*H*-Pyrrolo[2,3-b]pyridine-4-yl)methylamino)-5-fluoronicotinic Acid. *J. Org. Chem.* **2006**, *71*, 4021–4023.

(21) See Experimental Section for details.

(22) This result is consistent with the data previously reported for an analogous benzene C-ring series (IC_{50} = 0.004 μM with the propargyl group and IC_{50} = 0.087 μM without the propargyl group, i.e., a ~22-fold difference) (see ref 10).

(23) The direct (*S*)-propargyl-piperazine analogue of **51** was not prepared; however, the des-nitrogen version of **51** (i.e., phenyl C-ring) and its corresponding (*S*)-methyl-piperazine analogue were prepared and evaluated (see below). As illustrated below, the difference of activities between these two compounds in the AlphaScreen binding assay is striking (0.028 vs 5.5 μM). This data supports the assertion that the upper hydrophobic pocket and the shelf regions cannot be simultaneously occupied without engaging in a significant steric clash with the protein.

Y = 3'-Py, R = H
Y = 3'-Py, R = (S)-Me

hGK-hGKRP
AlphaScreen
IC_{50} = 0.028 μM
IC_{50} = 5.5 μM
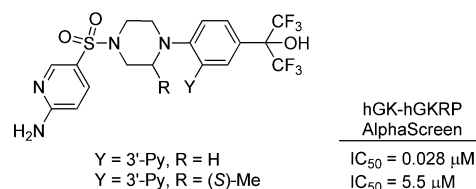
(24) Similar changes in Tyr24 and Pro29 residues were also observed in X-ray cocrystal structure with the 1-methyl-4-1*H*-pyrazole substituted analogue, **34**.

(25) For comparison, the efficacy of compound **1** is also reported (see Supporting Information).

(26) Note: Different methods were used to measure the exposure levels of compound **51** in the efficacy and pharmacodynamic experiments (Figure 7b vs Figure 7d). For Figure 7b, the whole blood was taken by a dry blood spot (DBS) technique at nonterminal time points, while for Figure 7d plasma samples were taken at terminal time points through a cardio puncture. Although lower exposure levels of compound **51** were observed in the pharmacodynamic study than were obtained in the efficacy study at 100 mg/kg, the unbound exposure levels were sufficient in both studies to cover the mouse EC_{50} value obtained from the GK translocation assay. For illustration, the unbound plasma concentrations of compound **51** from both the pharmocodynamic and efficacy studies are plotted on the same graph (see Supporting Information).

(27) Yu, S.; Li, S.; Yang, H.; Lee, F.; Wu, J.-T.; Qian, M. G. A Novel Lliquid Chromatography/Tandem Mass Spectrometry Based Depletion Method for Measuring Red Blood Cell Partitioning of Pharmaceutical Compounds in Drug Discovery. *Rapid Commun. Mass Spectrom.* **2005**, *19*, 250–254.